



**HAL**  
open science

# Genome galaxy identified by the circular code theory

Christian J Michel, Jean-Sébastien Sereni

► **To cite this version:**

Christian J Michel, Jean-Sébastien Sereni. Genome galaxy identified by the circular code theory. Bulletin of Mathematical Biology, 2024, 87 (5), 10.1007/s11538-024-01366-1 . hal-04574179v2

**HAL Id: hal-04574179**

**<https://hal.science/hal-04574179v2>**

Submitted on 13 Nov 2024

**HAL** is a multi-disciplinary open access archive for the deposit and dissemination of scientific research documents, whether they are published or not. The documents may come from teaching and research institutions in France or abroad, or from public or private research centers.

L'archive ouverte pluridisciplinaire **HAL**, est destinée au dépôt et à la diffusion de documents scientifiques de niveau recherche, publiés ou non, émanant des établissements d'enseignement et de recherche français ou étrangers, des laboratoires publics ou privés.



Distributed under a Creative Commons Attribution 4.0 International License

# Genome galaxy identified by the circular code theory

CHRISTIAN J. MICHEL\*, JEAN-SÉBASTIEN SERENI

*Theoretical Bioinformatics, ICube,  
C.N.R.S., University of Strasbourg,  
300 Boulevard Sébastien Brant  
67400 Illkirch, France*

*\*Corresponding author*

**ABSTRACT.** The genome galaxy identified in bacteria is studied by expressing the reading frame retrieval (RFR) function according to the  $YZ$ -content ( $GC$ -,  $AG$ - and  $GT$ -content) of bacterial codons. We have developed a simple probabilistic model for ambiguous sequences in order to show that the RFR function is a measure of the gene reading frame retrieval. Indeed, the RFR function increases with the ratio of ambiguous sequences and the ratio of ambiguous sequences decreases when the codon usage dispersion increases. The classical  $GC$ -content is the best parameter for characterizing the upper arm, which is related to bacterial genes with a low  $GC$ -content, and the lower arm, which is related to bacterial genes with a high  $GC$ -content. The galaxy center has a  $GC$ -content around 0.5. Then, these results are confirmed by expressing the  $GC$ -content of bacterial codons as a function of the codon usage dispersion. Finally, the bacterial genome galaxy is better described with the  $GC3$ -content in the 3rd codon site compared to the  $GC1$ -content and  $GC2$ -content in the 1st and 2nd codons sites, respectively.

Whereas the codon usage is used extensively by biologists, its dispersion, which is an important parameter to reveal this genome galaxy, is surprisingly little known and unused. Therefore, we have developed a mathematical theory of codon usage dispersion by deriving several formulæ. It shows three important parameters in codon usage: the minimum and maximum codon probabilities and the number of codons with high frequency, i.e. with a probability at least  $1/64$ . By applying this theory to the evolution of the genetic code, we see that bacteria have optimised the number of codons with high frequency to maximise the codon dispersion, thus maximising the capacity to retrieve the reading frame in genes. The derived formulæ of dispersion can be easily extended to any weighted code over a finite alphabet.

## 1. Introduction

Based on the circular code theory, a beautiful and intriguing “galaxy” structure has been identified in the genomes of bacteria, as well as of eukaryota and archaea [20]. This genome galaxy has a center and two arms, an upper one and a lower one, a structure that is identified for the three kingdoms [20, Figures 5, 7 and 8]. The aim of this work is to characterise this genome galaxy for bacteria.

The circular code theory has been initiated in 1996 by the identification in genes of bacteria and eukaryotes, of a maximal  $C^3$  self-complementary circular code, a particular set called  $X$  of 20 trinucleotides with interesting mathematical properties allowing to retrieve the reading frame

---

*E-mail address:* c.michel@unistra.fr, jean-sebastien.sereni@cnrs.fr.

*Date:* November 12, 2024.

*Key words and phrases.* genome galaxy; circular code theory; reading frame retrieval; probabilistic model for ambiguous sequences; formulas for codon usage; codon dispersion.

and the two shifted frames in genes [1]. In 2017, it has been shown that this circular code  $X$  is also found in genes of archaea, plasmids and viruses [12]. The historical context of this result is described in a recent article [13]. We also refer the reader to the reviews [9, 11] for the biological context and the main combinatorial studies of circular codes.

This unexpected biological result has led to several mathematical developments since 1996: (i) the flower automaton [1]; (ii) the necklaces  $LDN$  (letter diletter necklace) and  $DLN$  (diletter letter necklace) [17, 18, 23] extended to  $(n+1)LDCCN$  (letter diletter continued closed necklaces) [16]; (iii) the group theory [5]; and (iv) the recent and powerful approach based on graph theory in 2016 [8]. The graph approach has recently led to two important generalizations: mixed circular codes [6] and  $k$ -circular codes [7, 15, 19].

These theoretical results have led to biological applications, to name a few recent ones: identification of “universal” circular code motifs in the ribosome leading to a model of genetic code evolution associating codes, translation systems, and peptide products at different stages, from the primordial translation building blocks to the ancestor of the modern ribosome present in the Last Universal Common Ancestor (LUCA) [4]; identification of a circular code periodicity (modulo 3) in a large region of the 16S rRNA including the 3’ major domain corresponding to the primordial proto-ribosome decoding center, containing numerous sites that interact with the tRNA and mRNA during translation and surrounding the mRNA channel [21]; potential role of the circular code  $X$  in the regulation of gene expression [27]; and characterization of accessory genes in coronavirus genomes using the circular code information [14].

On the genetic alphabet, there are  $2^{64} - 1 \approx 10^{19}$  (non-empty) trinucleotide codes: 64 codes of cardinality 1 ( $\{AAA\}, \dots, \{TTT\}$ ); 2016 codes of cardinality 2 ( $\{AAA, AAC\}, \dots, \{TTG, TTT\}$ ); 41664 codes of cardinality 3 ( $\{AAA, AAC, AAG\}, \dots, \{TTC, TTG, TTT\}$ ); and so on up to 1 code of cardinality 64 (the genetic code  $\{AAA, \dots, TTT\}$ ). The recent theory of trinucleotide  $k$ -circular codes makes it possible to study the property of reading frame retrieval (RFR), called circularity property, for any of these  $\approx 10^{19}$  codes [15, 19].

The genome galaxy of bacteria will be analysed by the RFR function  $f$  (see Definition 2.13) that can be applied to the codon usage, and two codon parameters: dispersion (see Definition 2.7) and  $YZ$ -content (see Definition 2.9). The  $YZ$ -content of codon is a simple extension of the  $GC$ -content, a main parameter to study the codon usage bias (CUB) that influences different aspects of protein production [10] and has effects at many biological stages, including transcription [28], translation efficiency [25], mRNA stability [24], protein folding [3] and protein function [2] (recent review in [22]). In addition, from a theoretical point of view, our work puts for the first time the circular code theory with its RFR function  $f$  in relation to the codon usage with its  $GC$ -content.

This article is organised as follows. The necessary definitions and notation of trinucleotide codes, circular codes and their generalization to  $k$ -circular codes are gathered in Section 2.1. Section 2.2 defines the dispersion function of codon usage and states a proposition about its range. Section 2.3 defines the  $YZ$ -content. Section 2.4 defines the reading frame retrieval (RFR) function and states several propositions concerning its range and its particular value 1 associated with a uniform codon usage. Section 2.5 explains why the RFR function is a measure of the gene reading frame retrieval. Section 2.6 defines the parameters involved in our mathematical theory of codon usage dispersion. Section 2.7 describes the acquisition of codon usage for the genomes of bacteria from the codon statistics database (CSD) [26].

The results are presented in two main parts. Section 3 presents new statistical results of the bacterial genome galaxy. It is divided into three parts. Section 3.1 characterizes the genome

galaxy of bacteria with its center, its upper arm and its lower arm. Section 3.2 shows that one parameter, the  $YZ$ -content of codon, and mainly the  $GC$ -content, allows the identification of the three structures of the genome galaxy. Section 3.3 demonstrates that the dispersion of codon usage is mainly related to the  $GC$ -content of codon and that the  $GC3$ -content in the 3rd codon site is a main factor for the reading frame retrieval (RFR) function of genes.

Section 4 develops a mathematical study of codon usage dispersion, an analysis which, to our knowledge, has never been carried out. It is divided into two parts. Section 4.1 derives several formulæ of codon usage dispersion. Section 4.2 gives three applications of this mathematical study to the evolution of the bacterial genetic code. The maximum dispersion of the current genetic code at 64 codons is analysed as a function of its codon of maximum probability (Section 4.2.1) and that of minimum probability (Section 4.2.2). Moreover, Section 4.2.3 studies the minimum and maximum dispersions of the evolutionary genetic code as functions of its number of codons, from 1 to 64.

## 2. Method

**2.1. Definitions and notation.** For the reader's convenience, and to have this article self-contained, we here recall the most relevant notions. The theoretical aspects, with computer results, proofs, examples, remarks, illustrations and refinements are found in the articles [15, 19, 20].

We work with the *genetic alphabet*  $\mathcal{B} := \{A, C, G, T\}$ , which has cardinality 4. An element  $N$  of  $\mathcal{B}$  is called *nucleotide*. A *word* over the genetic alphabet is a sequence of nucleotides. A *trinucleotide* is a sequence of 3 nucleotides, that is, using the standard word-theory notation, an element of  $\mathcal{B}^3$ . If  $w = N_1 \cdots N_s$  and  $w' = N'_1 \cdots N'_t$  are two sequences of nucleotides of respective lengths  $s$  and  $t$ , then the *concatenation*  $w \cdot w'$  of  $w$  and  $w'$  is the sequence  $N_1 \cdots N_s N'_1 \cdots N'_t$  composed of  $s + t$  nucleotides.

Given a sequence  $w = N_1 N_2 \cdots N_s \in \mathcal{B}^s$  and an integer  $j \in \{0, 1, \dots, s - 1\}$ , the *circular  $j$ -shift* of  $w$  is the word  $N_{j+1} \cdots N_s N_1 \cdots N_j$ . Note that the circular 0-shift of  $w$  is  $w$  itself. A sequence  $w'$  of nucleotides is a *circular shift* of  $w$  if  $w'$  is the circular  $j$ -shift of  $w$  for some  $j \in \{0, 1, \dots, s - 1\}$ . The elements in  $\mathcal{B}^3$  can thus be partitioned into conjugacy classes, where the *conjugacy class* of a trinucleotide  $w \in \mathcal{B}^3$  is the set of all circular shifts of  $w$ .

**Definition 2.1.** Let  $\mathcal{B}$  be the genetic alphabet.

- A *trinucleotide code* is a subset of  $\mathcal{B}^3$ , that is, a set of trinucleotides.
- If  $X$  is a trinucleotide code and  $w$  is a sequence of nucleotides, then an  *$X$ -decomposition* of  $w$  is a tuple  $(x_1, \dots, x_t) \in X^t$  of trinucleotides from  $X$  such that  $w = x_1 \cdot x_2 \cdots x_t$ .

We now formally define the notion of circularity of a code, i.e. the property of reading frame retrieval (RFR).

**Definition 2.2.** Let  $X \subseteq \mathcal{B}^3$  be a trinucleotide code.

- Let  $m$  be a positive integer and let  $(x_1, \dots, x_m) \in X^m$  be an  $m$ -tuple of trinucleotides from  $X$ . A *circular  $X$ -decomposition* of the concatenation  $c := x_1 \cdots x_m$  is an  $X$ -decomposition of a circular shift of  $c$ .
- Let  $k$  be a non-negative integer. The code  $X$  is  $(\geq k)$ -*circular* if every concatenation of trinucleotides from  $X$  that admits more than one circular  $X$ -decomposition contains at least  $k + 1$  trinucleotides. In other words,  $X$  is  $(\geq k)$ -circular if for every  $m \in \{1, \dots, k\}$  and each  $m$ -tuple  $(x_1, \dots, x_m)$  of trinucleotides from  $X$ , the concatenation  $x_1 \cdots x_m$  admits a unique circular  $X$ -decomposition. The code  $X$  is  $k$ -*circular* if  $X$  is  $(\geq k)$ -circular and not  $(\geq k + 1)$ -circular.



- The code  $X$  is *circular* if it is  $(\geq k)$ -circular for all  $k \in \mathbf{N}$ .

We recall the definition of the graph associated with a trinucleotide code [8].

**Definition 2.3.** Let  $X \subseteq \mathcal{B}^3$  be a trinucleotide code. We define a graph  $\mathcal{G}(X) = (V(X), E(X))$  with set of vertices  $V(X)$  and set of arcs  $E(X)$  as follows:

- $V(X) := \bigcup_{N_1N_2N_3 \in X} \{N_1, N_3, N_1N_2, N_2N_3\}$ ; and
- $E(X) := \{N_1 \rightarrow N_2N_3 : N_1N_2N_3 \in X\} \cup \{N_1N_2 \rightarrow N_3 : N_1N_2N_3 \in X\}$ .

The graph  $\mathcal{G}(X)$  is the graph *associated* with  $X$ .

The *length* of a directed cycle in a graph  $\mathcal{G}$  is the number of arcs of the cycle. We note that every arc of  $\mathcal{G}(X)$  joins a nucleotide and a dinucleotide. Thus, the graph  $\mathcal{G}(X)$  cannot contain a directed cycle of odd length. A theorem [7, Theorem 3.3] implies that a cycle in  $\mathcal{G}(X)$ , if any, must have length in  $\{2, 4, 6, 8\}$  and, in particular, that a trinucleotide  $(\geq 4)$ -circular code must be circular. As noted in a previous article [15], it follows that all trinucleotide codes over  $\mathcal{B}$  can be naturally partitioned into 5 classes using the following definition.

**Definition 2.4.** We define the *circularity*  $\text{cir}(X)$  of a non-empty trinucleotide code  $X$  to be the largest integer  $k \in \{0, 1, 2, 3, 4\}$  such that  $X$  is  $(\geq k)$ -circular.

Thus, the possible values of  $\text{cir}(X)$  for a trinucleotide code  $X$  are 0, 1, 2, 3, 4, which determine the 5 classes.

Next we introduce two functions, which turn out to be correlated. The first one deals with the dispersion of the codon usage, and the second one, which uses the graph, deals with the property of reading frame retrieval (RFR) of genes. These two functions are also analysed as a function of the mean number of codons per gene in each genome.

**2.2. Dispersion of codon usage.** We recall the definition and the proposition of codon usage introduced in a previous work [20]. A codon usage is *uniform* if every codon has the same occurrence frequency. We shall introduce a function to measure the dispersion of codon usage with respect to the uniform one. We write  $X_g$  instead of  $\mathcal{B}^3$ , the particular code of cardinality 64 containing all trinucleotides, which is the well-known genetic code.

**Definition 2.5** (Codon usage). Given any trinucleotide code  $X$ , a *weight function on  $X$*  is a function  $\omega: X \rightarrow [0, 1]$  such that  $\sum_{x \in X} \omega(x) = 1$ .

**Definition 2.6.** A *weighted trinucleotide code* is a pair  $(X, \omega)$  where  $X$  is a trinucleotide code and  $\omega$  is a weight function on  $X$ .

We can now define the dispersion of codon usage.

**Definition 2.7** (Dispersion of codon usage, [20, Definition 2.8]). For every weight function  $\omega: X_g \rightarrow [0, 1]$ , the *dispersion of codon usage in  $(X_g, \omega)$*  is the function  $d$  given by

$$d((X_g, \omega)) = \sum_{x \in X_g} \left| \omega(x) - \frac{1}{64} \right|. \quad (2.1)$$

The next proposition gives the extremal values taken by the function  $d$ .

PROPOSITION 2.8 ([20, Proposition 2.9]). *For every weight function  $\omega: X_g \rightarrow [0, 1]$ , we have*

$$0 \leq d((X_g, \omega)) \leq \frac{63}{32} \approx 1.97.$$

Moreover,  $d((X_g, \omega)) = 0$  if and only if  $\omega(x) = \frac{1}{64}$  for each trinucleotide  $x \in X_g$ . The upper bound is attained if and only if there is a trinucleotide  $x \in X_g$  such that  $\omega(x) = 1$  (and hence  $\omega(x') = 0$  if  $x' \neq x$ ).

### 2.3. YZ-content.

**Definition 2.9.** Let  $n_A, n_C, n_G$  and  $n_T$  be the number of the nucleotide  $A, C, G$  and  $T$  of  $\mathcal{B}$  in the 3 codon sites. Let  $Y$  and  $Z$  be 2 different nucleotides of  $\mathcal{B}$ . Then the  $YZ$ -content is the probability

$$YZ\text{-content} = \frac{n_Y + n_Z}{N} \quad (2.2)$$

where  $N = n_A + n_C + n_G + n_T$ .

Note that the number of codons is  $N/3$ . Obviously,  $YZ$ -content =  $ZY$ -content and  $YZ$ -content +  $\bar{Y}\bar{Z}$ -content = 1 where the complementary nucleotide  $\bar{N}$  of a nucleotide  $N \in \mathcal{B}$  is given by  $\bar{A} = T, \bar{T} = A, \bar{C} = G$  and  $\bar{G} = C$ . The classical biological parameter is the  $GC$ -content. In this work, we will also study the parameters  $AG$ -content and  $GT$ -content.

The definition of the  $YZ$ -content can easily be generalized to  $YZk$ -content associated with the  $k$ th codon site where  $k \in \{1, 2, 3\}$ . Note that, using the above notation, the normalisation factor (i.e., the denominator) is not  $N$  but  $N/3$ , i.e. the number of codons. The classical biological parameter is the  $GC3$ -content. In this work, we will also study the parameters  $GC1$ -content and  $GC2$ -content.

### 2.4. Gene reading frame retrieval (RFR) function associated with a codon usage.

Theoretical considerations over trinucleotide codes led to the following definition [19, Definition 6.1] as a measure of the reading frame retrieval of genes. Indeed, the number and length of cycles in the graph are associated with ambiguous sequences that do not retrieve the reading frame. Short cycles are associated with short ambiguous sequences, i.e. the reading frame is lost quickly (e.g., after 1 trinucleotide), in contrast to long cycles where the ambiguous sequences are long, i.e. the reading frame is lost after several trinucleotides, up to 4 trinucleotides (see [15, 19] for details). We will explain this important property in detail in the following Section 2.5.

**Definition 2.10** ([19, Definition 6.1]). The *reading frame loss* function  $f$  of a trinucleotide code  $X$  is the mapping  $f: \mathcal{B}^3 \rightarrow \mathbf{R}$  given by

$$f(X) := q_8(\mathcal{G}(X)) + \frac{4}{3} q_6(\mathcal{G}(X)) + 2 q_4(\mathcal{G}(X)) + 4 q_2(\mathcal{G}(X)) = \sum_{i=1}^4 \frac{4}{i} \cdot q_{2 \cdot i}(\mathcal{G}(X)) \quad (2.3)$$

where  $q_i(\mathcal{G})$  is the number of directed cycles of length  $i$  in the graph  $\mathcal{G}$  for every positive integer  $i$ .

The next proposition gives the minimum and maximum values taken by  $f$  over all trinucleotide codes.

**PROPOSITION 2.11** ([19, Proposition 6.2]). *For every trinucleotide code  $X$ , we have  $0 \leq f(X) \leq 301056$ . Moreover,  $f(X) = 0$  if and only if  $X$  is a trinucleotide circular code, and  $f(X) = 301056$  if and only if  $X$  is the genetic code  $X_g$ , where*

$$q_2(X_g) = 64, \quad q_4(X_g) = 1440, \quad q_6(X_g) = 26880, \quad q_8(X_g) = 262080.$$

The function  $f$  generalises to the codon usage, where each trinucleotide  $x$  has occurrence frequency  $w(x)$ .

**Definition 2.12** ([20, Definition 2.12]). Let  $(X, \omega)$  be a weighted trinucleotide code. The *weighted graph associated with  $\omega$*  is the pair  $(\mathcal{G}(X), \omega')$  where  $\mathcal{G}(X)$  is given by Definition 2.3 with respect to  $X$ , and  $\omega'$  is a function assigning to each of the two arcs of  $\mathcal{G}(X)$  coming from a trinucleotide  $N_1N_2N_3 \in X$  the rational number  $\frac{\omega(N_1N_2N_3)}{2} \in [0, 1]$ .

In other words, the arcs of the weighted graph  $(\mathcal{G}(X), \omega')$  can be written as follows:

$$\left\{ N_1 \xrightarrow{\omega(x)/2} N_2N_3 : x = N_1N_2N_3 \in X \right\} \cup \left\{ N_1N_2 \xrightarrow{\omega(x)/2} N_3 : x = N_1N_2N_3 \in X \right\}.$$

The generalised function  $f$  associated with every weighted trinucleotide code that has identified the genome galaxy in bacteria, archaea and eukaryota, has been defined as follows.

**Definition 2.13** ([20, Definition 2.13]). Let  $(X, \omega)$  be a weighted trinucleotide code and  $(\mathcal{G}(X), \omega')$  its associated weighted graph. Let  $\mathcal{C}$  be the set of all directed cycles of  $\mathcal{G}(X)$ . The *loss of reading frame retrieval (RFR)* function  $f$  of  $(X, \omega)$  is the mapping  $f$  given by

$$f((X, \omega)) := \frac{1}{|\mathcal{C}|} \sum_{c \in \mathcal{C}} (2|X|)^{|c|} \prod_{a \in E(c)} \omega'(a) \quad (2.4)$$

where  $E(c)$  is the set of arcs of the directed cycle  $c$ .

For the convenience of the reader, we recall three propositions (without proof).

**PROPOSITION 2.14** (Uniform codon usage, [20, Proposition 2.14]). *Let  $X_g$  be the genetic code and let  $\omega$  the uniform distribution over  $X_g$ , that is,  $\omega : X_g \rightarrow [0, 1]$  is constant and equal to  $\frac{1}{64}$ . Then  $f((X_g, \omega)) = 1$ .*

The next proposition implies that for circular codes, the weight function  $\omega$  has no significance for  $f$ , in the sense that all distributions yield the same value as the uniform one, namely 0.

**PROPOSITION 2.15** (Circular code, [20, Proposition 2.15]). *Let  $(X, \omega)$  be a weighted trinucleotide code. Then  $f((X, \omega)) = 0$  if and only if  $X$  is a circular code.*

The function  $f$  seems to be maximised by codes obtained from a circular code of maximal size (20) by adding a periodic trinucleotide  $x$  (i.e.  $AAA$ ,  $CCC$ ,  $GGG$  or  $TTT$ ), with a weight function tending to 1 on  $x$  and 0 on all other trinucleotides, leading to the following observation.

**PROPOSITION 2.16** ([20, Proposition 2.16]). *We have*

$$\sup\{f(X, \omega) : (X, \omega) \text{ weighted trinucleotide code}\} \geq 441.$$

*That is, for every  $\varepsilon > 0$ , there exists a weighted trinucleotide code  $(X, \omega)$  such that  $f(X, \omega) > 441 - \varepsilon$ .*

**2.5. Probabilistic model for ambiguous sequences.** The RFR function of a weighted trinucleotide code is associated with the ambiguous sequences that do not retrieve the reading frame. In order to demonstrate this property, we describe a simple probabilistic model  $\mathcal{M}_1$  to quantify the capacity of a weighted trinucleotide code to retrieve the reading frame.

Let  $(X_g, \omega)$  be a weighted trinucleotide code, where, as already mentioned,  $X_g$  is the genetic code of cardinality  $|X_g| = 64$ . Real-life genomes usually comprise all 64 codons. So we assume that  $w$  is positive, i.e.  $w(x) > 0$  for each  $x \in X_g$ . As a consequence, every sequence of codons is ambiguous, i.e. it can be read in all 3 frames when written on a circle. We use the codon frequency of the sequences to quantify whether a sequence and its circular shifts can be identified, or not, as being in reading frame. Let us formalize this problem.

We fix a positive length  $m$  and consider all sequences (concatenations) composed of  $m$  trinucleotides of  $X_g$ , that is all sequences of  $s = 3m$  nucleotides (as defined in Section 2.1). We want to determine the probability of detection error between any given sequence  $w = N_1 \cdots N_s$  composed of  $s$  nucleotides (hence  $m$  trinucleotides) and its circular 1-shift  $w_1 = N_2 \cdots N_s N_1$ . We consider this case appears when at least one of the sequences  $w$  and  $w_1$  occurs frequently enough and the discrepancy between their two codon frequencies is not too large. These conditions depend on the weight  $\omega$ , i.e. the codon usage. This approach is based on the two following observations:

- Observation (i) if both  $w$  and  $w_1$  have a low probability of occurring (i.e., under an arbitrarily fixed threshold) then an error on their reading frame does not occur often, and thus could be considered biologically insignificant; and
- Observation (ii) if one of them, say  $w_1$  for instance, occurs much less frequently than  $w$ , then it is certain to consider the reading frame of  $w$  rather than that of  $w_1$ , since this frame will be “almost always” correct.

Consequently, every such couple  $(w, w_1)$  in these two cases is considered not to represent a problematic ambiguity regarding the reading frame.

We now define the codon frequency of the sequence  $w = N_1 \cdots N_s$  composed of the  $m$  codons  $x_i = N_{3i+1}N_{3i+2}N_{3i+3}$  for each  $i \in \{0, \dots, m-1\}$ . The probability of a codon  $x \in X_g$  is directly given by the weight function  $\omega$ . By assuming independence of the codon frequencies within a sequence, then the probability  $p(w)$  of  $w$  is

$$p(w) = \prod_{i=0}^{m-1} \omega(x_i). \quad (2.5)$$

Fix two reals  $\varepsilon > 0$  and  $R > 1$ , which will be used as a threshold and a ratio bound, respectively. For each such sequence  $w$ , we compute its probability  $p(w)$  and the probability  $p(w_1)$  of its circular 1-shift  $w_1$ . We say these two sequences  $w$  and  $w_1$  are *ambiguous* if:

$$\begin{aligned} (1) \quad & p(w) > \varepsilon \text{ and } p(w_1) > \frac{p(w)}{R}; \text{ or} \\ (2) \quad & p(w_1) > \varepsilon \text{ and } p(w) > \frac{p(w_1)}{R}. \end{aligned} \quad (2.6)$$

When none of these two cases occurs, we consider the sequences to be not ambiguous as explained earlier (see [Observation \(i\)](#) and [Observation \(ii\)](#)).

We additionally note that the condition to declare  $w$  and  $w_1$  ambiguous is symmetric with respect to  $w$  and  $w_1$ . Therefore, it is enough to consider circular 1-shifts. Indeed, with sequences of trinucleotides, if  $w_2$  is the circular 2-shift of  $w$ , then  $w$  is the circular 1-shift of  $w_2$ , so that the pair  $\{w, w_2\}$  will be dealt with anyway.

**Example 2.17.** We use the (average) codon usage of  $X_g$  provided in Appendix Table 1 to define  $\omega$ , so  $\omega(AAA) = 0.0237$  and  $\omega(TTT) = 0.0161$  for instance. Consider the sequence  $w = AAA \cdot AAC \cdot AAG$  composed of  $m = 3$  codons. The probability of  $w$  is  $p(w) = \omega(AAA) \times \omega(AAC) \times \omega(AAG) = 0.0237 \times 0.0180 \times 0.0200 \approx 8.5 \times 10^{-6}$ . The circular 1-shift of  $w$  is the sequence  $w_1 = AAA \cdot ACA \cdot AGA$ , and hence  $p(w_1) = \omega(AAA) \times \omega(ACA) \times \omega(AGA) = 0.0237 \times 0.0093 \times 0.0054 \approx 1.2 \times 10^{-6}$ .

Suppose, for example, that the threshold is  $\varepsilon = \frac{1}{|X_g|^3} = \frac{1}{64^3} \approx 3.8 \times 10^{-6}$  and the ratio bound is  $R = 10$ . We then see that  $p(w) > \varepsilon$  and in addition that  $p(w_1) > \frac{p(w)}{10}$ . Therefore with these parameters the sequences  $w$  and  $w_1$  are ambiguous according to (2.6).

We perform the above test (2.6) for all sequences of  $m$  trinucleotides, giving us the number  $a$  of ambiguous pairs. The normalisation of  $a$  by dividing it by the total number  $|X_g|^m$  of

such sequences, leads to the ratio  $r$  (rational number in  $[0, 1]$ ) of ambiguous sequences (of  $m$  trinucleotides) for the weighted trinucleotide code  $(X_g, \omega)$

$$r = \frac{a}{|X_g|^m} = \frac{a}{64^m}. \quad (2.7)$$

This ratio  $r$  can be interpreted as the probability that a sequence of  $m$  consecutive trinucleotides is ambiguous, meaning that there is a significant detection error of the reading frame.

**Remark 2.18.** There is no unique model to quantify the reading frame retrieval capacity of all the bacterial genomes. A 2nd model  $\mathcal{M}_2$  can consider a “shifted” codon usage of sequences in a shifted frame. Given a sequence  $w$  and its circular 1-shift  $w_1$ , the probability that  $w_1$  occurs *in reading frame 1* can be computed using probabilities obtained by shifting the original (i.e. frame 0) codon usage. Specifically, the weight  $\omega_1$  for each trinucleotide  $N_1N_2N_3 \in X_g$  is defined as follows:

$$\omega_1(N_1N_2N_3) = \left( \sum_{N \in \mathcal{B}} \omega(NN_1N_2) \right) \cdot \left( \sum_{N', N'' \in \mathcal{B}} \omega(N_3N'N'') \right). \quad (2.8)$$

Indeed,  $N_1N_2N_3$  is read in frame 1 if and only if  $NN_1N_2 \cdot N_3N'N''$  is read in frame 0 for some  $N, N', N'' \in \mathcal{B}$ . The probability of a given concatenation  $w = N_1 \cdots N_s$  of  $s = 3m$  nucleotides then depends on the position of the sequence with respect to the actual reading frame: if this sequence occurs in frame 0 then the probability is, as before,  $p(w) = \prod_{i=1}^m \omega(x_i)$ , while if it occurs in frame 1 then the probability becomes  $p_1(w) = \prod_{i=1}^m \omega_1(x_i)$ . Using conditions analogous to (2.6), the model  $\mathcal{M}_2$  recovers results similar to the model  $\mathcal{M}_1$  (not shown to avoid overloading the content).

Finally, a 3rd model  $\mathcal{M}_3$  can also be based on  $p_2(w)$  by shifting the 1-frame codon usage. Then,  $w$  can be considered unambiguous if one of the 3 probabilities  $p(w)$ ,  $p_1(w)$  and  $p_2(w)$  is “significantly greater” than the other two. But in this case, as almost all sequences are ambiguous, the use of a threshold (similar to **Observation (i)**) is necessary. The model  $\mathcal{M}_3$  finds similar results to the previous models  $\mathcal{M}_1$  and  $\mathcal{M}_2$  (not shown).

The ratio  $r$  (2.7) of ambiguous sequences will be computed in Sections 3.1.2, 3.1.3 and 3.2 on all sequences of  $m = 4$  trinucleotides with the threshold  $\varepsilon = \frac{1}{10 \cdot 64^4}$  and the ratio bound  $R = 10$ . We have also performed computer calculations on shorter and longer sequences (namely  $m = 3$  and  $m = 5$ ) with the corresponding threshold (i.e.  $\varepsilon = \frac{1}{10 \cdot 64^m}$ ) and obtained similar results (not shown). Other thresholds and ratio bounds were also analysed (in particular  $\varepsilon = \frac{1}{64^m}$ ), and they led to similar results (similar shapes, only scaled along to the  $x$ -axis; not shown).

**2.6. Parameters of a codon usage.** Given a codon usage, or equivalently a weighted trinucleotide code  $\mathcal{W} = (X_g, \omega)$  over the genetic code  $X_g$ , we retain several parameters that seem to influence in a non-trivial way the gene reading frame retrieval (RFR) function.

First, we discriminate between the trinucleotides that occur, and those that do not — or are so rare that are considered not to occur. Second, over these trinucleotides, we retain the lowest and the highest possible value of  $\omega$ , and also the number of trinucleotides with “high frequency”.

**Definition 2.19.** Let  $\mathcal{W} = (X_g, \omega)$  be a weighted trinucleotide code. We define

- (1)  $p_M(\mathcal{W}) = \max \{ \omega(x) : x \in X_g \}$ ;
- (2)  $p_m(\mathcal{W}) = \min \{ \omega(x) : x \in X_g \text{ and } \omega(x) > 0 \}$ ;
- (3) the number  $n(\mathcal{W})$  of trinucleotides  $x$  that occur, that is such that  $\omega(x) > 0$ ; and
- (4) the number  $n_h(\mathcal{W})$  of trinucleotides  $x$  of *high frequency*, that is such that  $\omega(x) \geq \frac{1}{n(\mathcal{W})}$ .

**2.7. Data.** From the codon statistics database (CSD, <http://codonstatsdb.unr.edu>) [26], we have extracted (July 2022) the codon usage of genomes of bacteria from the union of the 22 following bacterial classes: Acidobacteria (Id 57723), Actinobacteria (Id 201174), Aquificae (Id 187857), Bacteroidetes (Id 976), Balneolia (Id 1853221), Chlamydia (Id 204429), Chloroflexi (Id 200795), Cyanobacteria (Id 1117), Deferribacteres (Id 68337), Deinococcus-Thermus (Id 1297), Epsilonproteobacteria (Id 29547), Firmicutes (Id 1239), Fusobacteria (Id 32066), Mycoplasmatales (Id 2085), Nitrospirae (Id 40117), Planctomycetes (Id 203682), Pseudomonadales (Id 72274), Spirochaetes (Id 203691), Synergistetes (Id 508458), Thermodesulfobacteria (Id 200940), Thermotogae (Id 200918) and Verrucomicrobia (Id 74201). The few exceptional genomes in which the codon usage of the stop codons is not given, are not considered. Thus, the bacterial kingdom contains 8,345 genomes, 34,020,997 genes and 11,087,876,805 codons.

The calculus of the codon usage in this bacterial kingdom is given in Appendix Table 1.

### 3. Statistical study of the bacterial genome galaxy

#### 3.1. Identification of the genome galaxy of bacteria.

3.1.1. *Gene reading frame retrieval (RFR) function according to the dispersion function.* By expressing the gene reading frame retrieval (RFR) function  $f$  (2.4) according to the dispersion function  $d$  (2.1) of codon usage in the bacterial genomes, a “genome galaxy” with a center and two arms has been identified in a previous work [20, Figure 5, Section 3.2]. By using the linear regression  $y = -1.35881x + 1.37993$  between  $d$  and  $f$  (with a Spearman rank correlation coefficient  $\rho = -0.83$  and  $p$ -value  $< 10^{-180}$ ), we characterize in this work these 3 structures. The galaxy center  $\mathcal{GC}$  is defined by the bacterial genomes such that

$$\mathcal{GC} := d \leq 0.6. \quad (3.1)$$

The upper arm  $\mathcal{GUA}$  is defined by the bacterial genomes such that

$$\mathcal{GUA} := \begin{cases} d > 0.6 \\ f > y \\ f > 0.2. \end{cases} \quad (3.2)$$

The lower arm  $\mathcal{GLA}$  is defined by the bacterial genomes such that

$$\mathcal{GLA} := \begin{cases} f < y & \text{if } d \in ]0.6, 0.9] \\ f < 0.2 & \text{if } d > 0.9. \end{cases} \quad (3.3)$$

Figure 1 describes this genome galaxy of bacteria with its center  $\mathcal{GC}$  (3.1) in blue, its upper arm  $\mathcal{GUA}$  (3.2) in green and its lower arm  $\mathcal{GLA}$  (3.3) in violet.

Several parameters are now investigated to analyse this codon dispersion. Surprisingly, in a next section, one parameter, the  $YZ$ -content of codon (Section 2.3), allows the identification of the three structures of the genome galaxy.

3.1.2. *Gene reading frame retrieval (RFR) function according to the ratio of ambiguous sequences.* By expressing the gene reading frame retrieval (RFR) function  $f$  (2.4) according to the ratio  $r$  (2.7) of ambiguous sequences, Figure 2 shows that the RFR function increases with the ratio of ambiguous sequences. Figure 2 is a “mirror image” of Figure 1.

3.1.3. *Ambiguous sequences according to the codon usage dispersion.* By expressing the ratio  $r$  (2.7) of ambiguous sequences according to the codon usage dispersion  $d$  (2.1), Figure 3 shows that the ratio of ambiguous sequences decreases when the codon usage dispersion increases. The dispersion of codon usage and the ratio of ambiguous sequences vary in opposite direction.



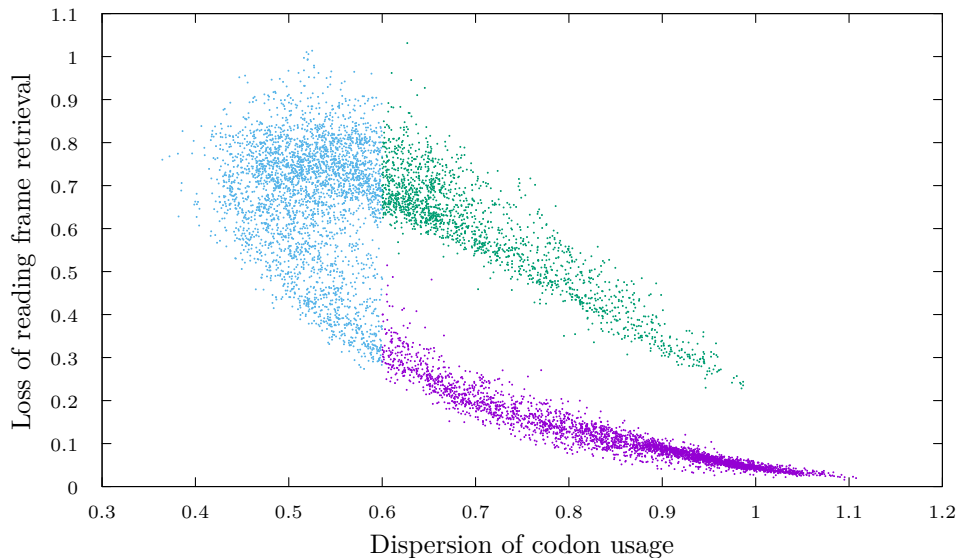


FIGURE 1. Genome galaxy of bacteria (8,345 genomes, 34,020,997 genes, 11,087,876,805 codons) with its center  $\mathcal{GC}$  (3.1) in blue, its upper arm  $\mathcal{GUA}$  (3.2) in green and its lower arm  $\mathcal{GLA}$  (3.3) in violet. Each point represents all the genes of a bacterial genome. The  $x$ -axis shows the dispersion function  $d$  (2.1) of codon usage. The  $y$ -axis shows the reading frame retrieval function  $f$  (2.4).

**Remark 3.1.** It is very interesting to stress that the two arms of the bacterial genome galaxy could be identified thanks to the RFR function function  $f$  (2.4) but not by the ratio  $r$  (2.7) of ambiguous sequences (compare Figures 1 and 3).

**3.2. Genome galaxy of bacteria identified by the  $GC$ -content of codon.** By expressing the gene reading frame retrieval (RFR) function  $f$  (2.4) according to the  $GC$ -content of codon, the 3 structures: center  $\mathcal{GC}$  (3.1), upper arm  $\mathcal{GUA}$  (3.2) and lower arm  $\mathcal{GLA}$  (3.3) are well characterized in Figure 4(A). The variation of the  $GC$ -content is important and in the interval  $[0.2, 0.8]$ . Note that,  $AT$  being complementary to  $GC$ , the  $AT$ -content leads to a symmetrical figure with respect to  $y = 0.5$  (not shown). Thus, the upper arm is related to genomes with a low  $GC$ -content while the lower arm is related to genomes with a high  $GC$ -content, the center being related to genomes with a  $GC$ -content around 0.5.

The variation of the  $AG$ -content (or equivalently  $GA$ -content as already mentioned) is restricted to the interval  $[0.45, 0.60]$ . The upper and lower arms are still separated but to a lesser extent (Figure 4(B)).

The variation of the  $GT$ -content is restricted to the interval  $[0.45, 0.55]$ . The upper and lower arms are neighbours (Figure 4(C)). Thus, the  $GT$ -content is not a parameter for characterizing the genome galaxy.

**3.3. Dispersion of codon usage related to the  $GC$ -content of codon.** According to the previous results, it is natural to express the dispersion function  $d$  (2.1) of codon usage in the bacterial genomes according to their  $YZ$ -content of codon (Section 2.3). Figure 5(A) confirms that the  $GC$ -content better identifies the three structures of the galaxy compared to the  $AG$ -content (Figure 5(B)) and the  $GT$ -content (Figure 5(C)).

By expressing the  $GC$ -content of codon according to the ratio  $r$  (2.7) of ambiguous sequences, Figure 6 is, as expected, a “mirror image” of Figure 5(A).



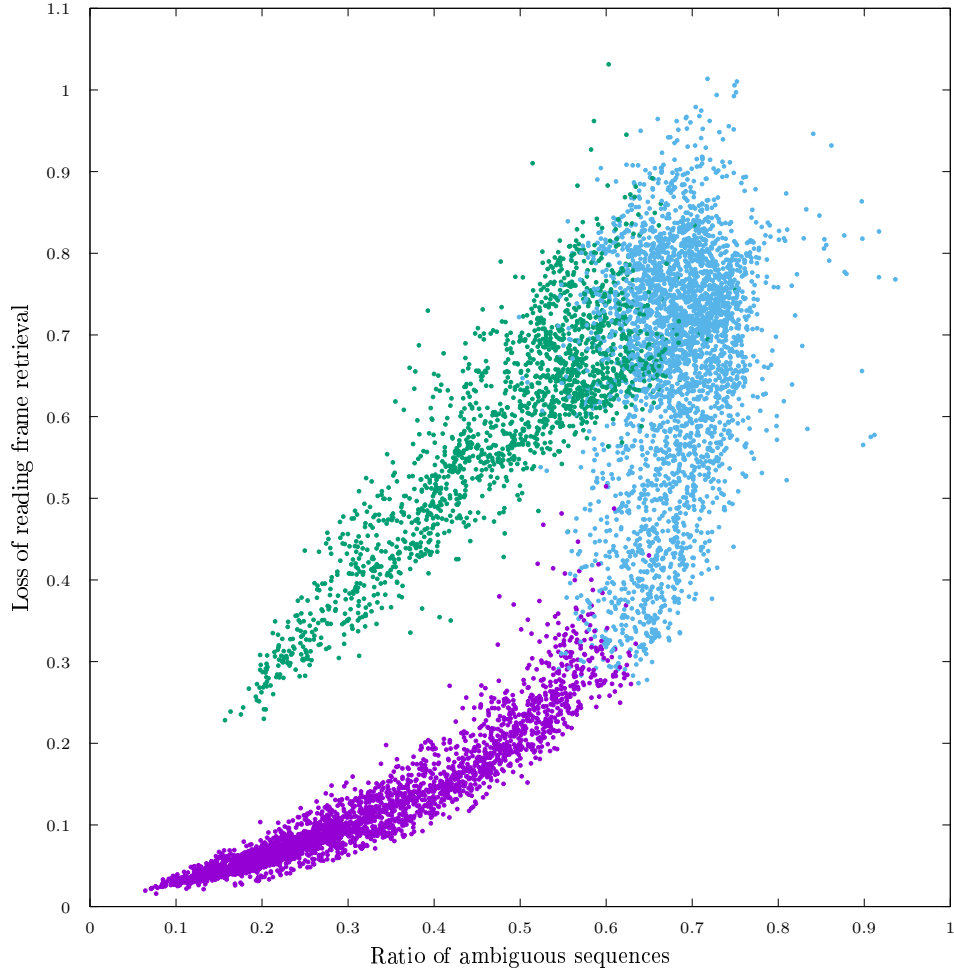


FIGURE 2. Genome galaxy of bacteria (8,345 genomes, 34,020,997 genes, 11,087,876,805 codons) with its center  $\mathcal{GC}$  (3.1) in blue, its upper arm  $\mathcal{GUA}$  (3.2) in green and its lower arm  $\mathcal{GLA}$  (3.3) in violet. Each point represents all the genes of a bacterial genome. The  $x$ -axis shows the ratio  $r$  (2.7) of ambiguous sequences. The  $y$ -axis shows the reading frame retrieval function  $f$  (2.4).

In order to further analyse the results with the  $GC$ -content, we express the gene reading frame retrieval (RFR) function  $f$  (2.4) according to  $GC$ -content in each of the 3 codon sites. The three galaxy structures are well characterized with the  $GC3$ -content in the 3rd codon site (Figure 7(C)). The variation of the  $GC3$ -content covers almost the entire interval  $[0.1, 1]$ . The upper arm is related to genomes with a low  $GC3$ -content while the lower arm is related to genomes with a high  $GC3$ -content, the center being related to genomes with a  $GC3$ -content around 0.5.

The variation of the  $GC1$ -content is restricted to the interval  $[0.30, 0.80]$ . The upper and lower arms are still separated but to a lesser extent (Figure 7(A)).

The variation of the  $GC2$ -content is restricted to the interval  $[0.25, 0.55]$ . The upper and lower arms are separated but close (Figure 7(B)).

In summary, the genome galaxy of bacteria with its center  $\mathcal{GC}$ , its upper arm  $\mathcal{GUA}$  and its lower arm  $\mathcal{GLA}$  is mainly related to the  $GC$ -content of codon, compared to the  $AG$ -content and the  $GT$ -content, and in particular to the  $GC3$ -content in the 3rd codon site, compared to the  $GC1$ -content and  $GC2$ -content.

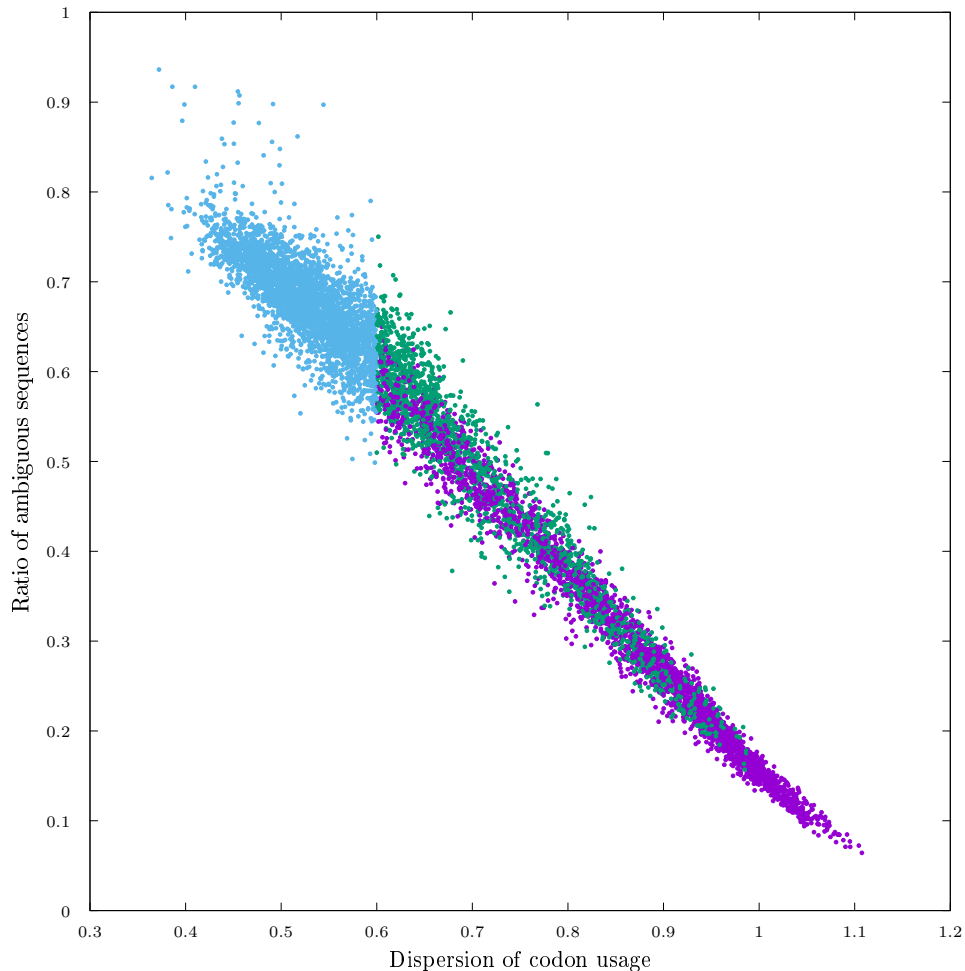


FIGURE 3. Genome galaxy of bacteria (8,345 genomes, 34,020,997 genes, 11,087,876,805 codons) with its center  $\mathcal{GC}$  (3.1) in blue, its upper arm  $\mathcal{GUA}$  (3.2) in green and its lower arm  $\mathcal{GLA}$  (3.3) in violet. Each point represents all the genes of a bacterial genome. The  $x$ -axis shows the dispersion function  $d$  (2.1) of codon usage. The  $y$ -axis shows the ratio  $r$  (2.7) of ambiguous sequences.

#### 4. A mathematical study of codon usage dispersion

Codon usage, i.e. the association of probabilities (frequencies) (Definition 2.5) with the 64 codons, is a biological parameter that has been the most widely studied and published. Surprisingly, the dispersion of codon usage (Definition 2.7) is a basic statistical parameter which, as far as we know, has been completely ignored in biology. This section is divided into two parts. In the first part, we develop a mathematical theory of dispersion by deriving various formulæ. In the second part, we apply this theory to the evolution of the genetic code. In particular, we address the following problem. In the current genetic code, not all 64 codons code for amino acids. Indeed, there are 3 unused codons, precisely the 3 stop codons  $\{TAA, TAG, TGA\}$ , with a probability equal to (close to) 0. The hypothesis that the genetic code evolves with the appearance of codons, i.e. with a non-zero probability, over time will therefore be studied.

**4.1. Formulæ of codon usage dispersion.** We study the dispersion of the weighted trinucleotide codes  $\mathcal{W} = (X_g, \omega)$  over the genetic alphabet  $X_g$  that satisfy certain properties. According to Definitions 2.6 and 2.19, we must have  $p_M(\mathcal{W}) \geq \frac{1}{n(\mathcal{W})}$  and  $p_m(\mathcal{W}) \leq \frac{1}{n(\mathcal{W})}$ . To

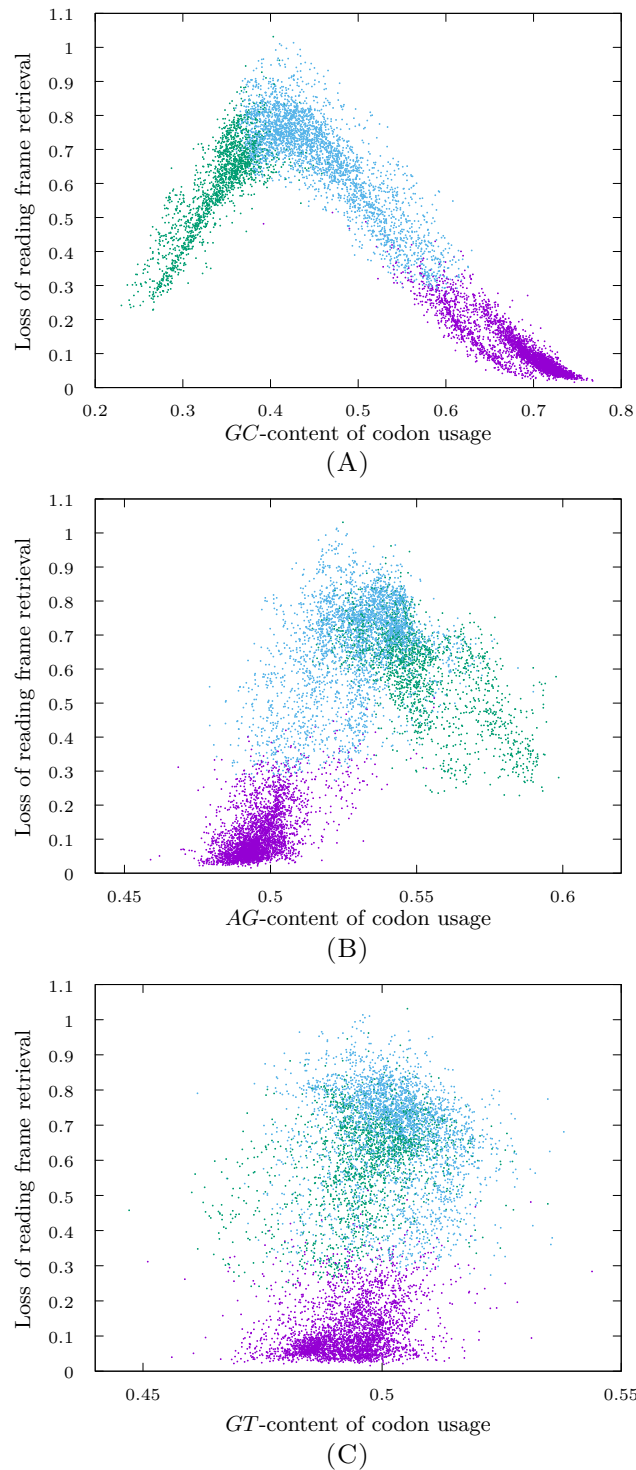


FIGURE 4. Genome galaxy of bacteria (8,345 genomes, 34,020,997 genes, 11,087,876,805 codons) with its center  $\mathcal{GC}$  (3.1) in blue, its upper arm  $\mathcal{GUA}$  (3.2) in green and its lower arm  $\mathcal{GLA}$  (3.3) in violet, identified by the  $YZ$ -content of codon, and mainly by the  $GC$ -content. Each point represents all the genes of a bacterial genome. The  $y$ -axis shows the reading frame retrieval function  $f$  (2.4). The  $x$ -axis shows the  $YZ$ -content of codon in the 3 cases: (A)  $GC$ -content; (B)  $AG$ -content; (C)  $GT$ -content.

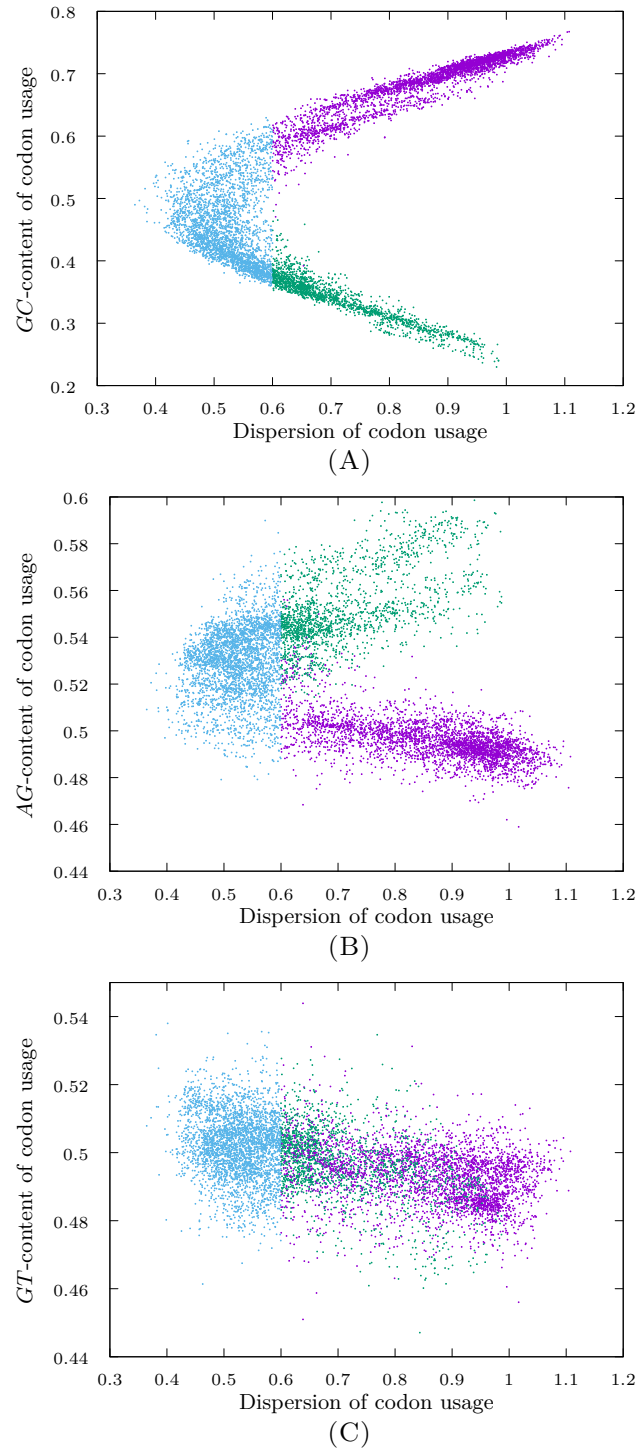


FIGURE 5. Genome galaxy of bacteria (8,345 genomes, 34,020,997 genes, 11,087,876,805 codons) with its center  $\mathcal{GC}$  (3.1) in blue, its upper arm  $\mathcal{GUA}$  (3.2) in green and its lower arm  $\mathcal{GLA}$  (3.3) in violet, identified by the  $YZ$ -content of codon, and mainly by the  $GC$ -content. Each point represents all the genes of a bacterial genome. The  $x$ -axis shows the dispersion function  $d$  (2.1) of codon usage. The  $y$ -axis shows the  $YZ$ -content of codon in the 3 cases: (A)  $GC$ -content; (B)  $AG$ -content; (C)  $GT$ -content.

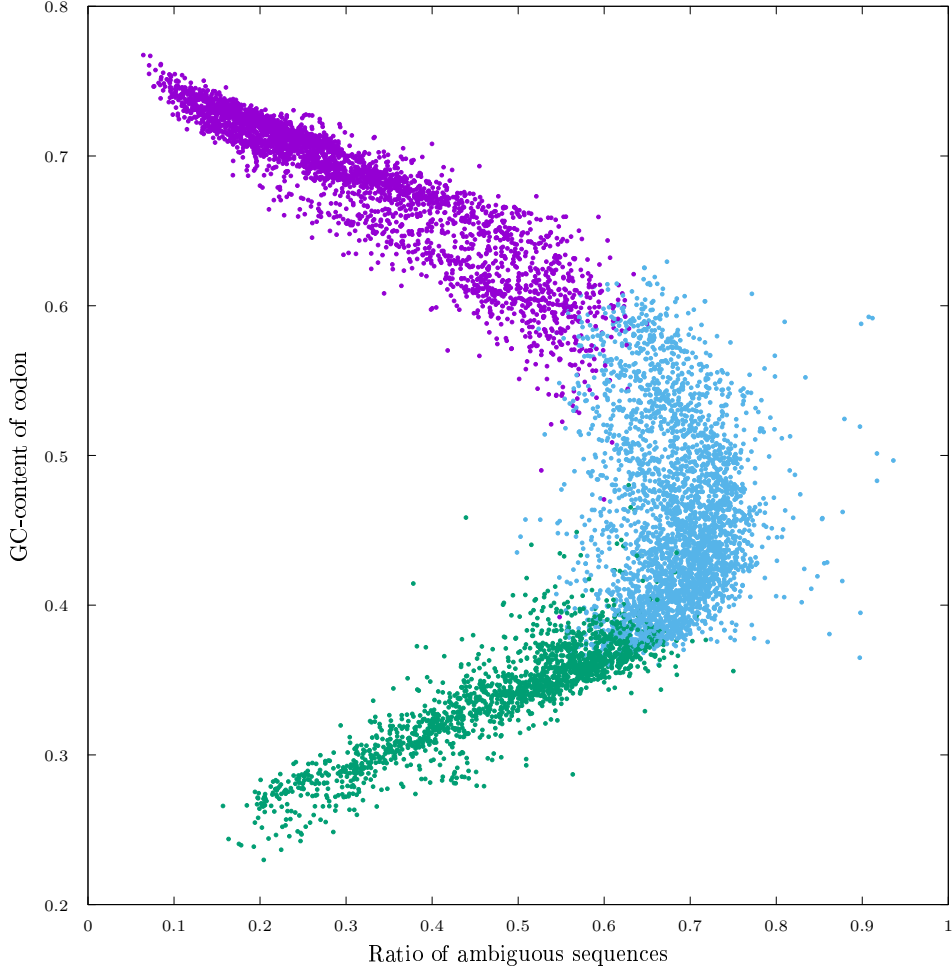


FIGURE 6. Genome galaxy of bacteria (8,345 genomes, 34,020,997 genes, 11,087,876,805 codons) with its center  $\mathcal{GC}$  (3.1) in blue, its upper arm  $\mathcal{GUA}$  (3.2) in green and its lower arm  $\mathcal{GLA}$  (3.3) in violet. Each point represents all the genes of a bacterial genome. The  $x$ -axis shows the ratio  $r$  (2.7) of ambiguous sequences. The  $y$ -axis shows the  $GC$ -content of codon.

ease the exposition, we consider an arbitrary enumeration  $x_1, \dots, x_{64}$  of  $X_g$ , and set  $\omega_i = \omega(x_i)$ . Accordingly, any weighted trinucleotide code over  $X_g$  can be viewed as the data of 64 non-negative real numbers summing to 1. We use this identification in the sequel.

We want to fix the number of trinucleotides that occur, the number of those of high frequency, and bounds on the minimum and maximum frequencies. To this end, we fix integers  $n \in \{1, \dots, 64\}$  and  $n_h \in \{1, \dots, n\}$ , along with positive real numbers  $p_m, p_M$  such that  $p_m \leq \frac{1}{n} \leq p_M$ . Indeed, if each of the  $n$  trinucleotides that occur has frequency at most  $p_M$ , then  $n \cdot p_M \geq 1$ , since  $n \cdot p_M \geq \sum_{i=1}^{64} \omega_i = 1$ . Similarly, if each of the  $n$  trinucleotides that occur has frequency at least  $p_m$ , then necessarily  $n \cdot p_m \leq 1$ . Furthermore, at least one trinucleotide must have frequency at least  $\frac{1}{n}$ , so we always assume that  $n_h \geq 1$ . We note that for every  $n_h \in \{1, \dots, n-1\}$ ,

$$n \cdot p_m \leq 1 \Leftrightarrow p_m \leq \frac{1}{n} \Leftrightarrow (n - n_h) \cdot p_m \leq \frac{n - n_h}{n} \Leftrightarrow \frac{n_h}{n} + (n - n_h) \cdot p_m \leq 1.$$

We consider only trinucleotide codes satisfying the following three conditions:

- (1) for every  $i \in \{1, \dots, n_h\}$  we have  $\frac{1}{n} \leq \omega_i \leq p_M$ ;
- (2) for every  $i \in \{n_h + 1, \dots, n\}$  we have  $p_m \leq \omega_i \leq \frac{1}{n}$ ; and

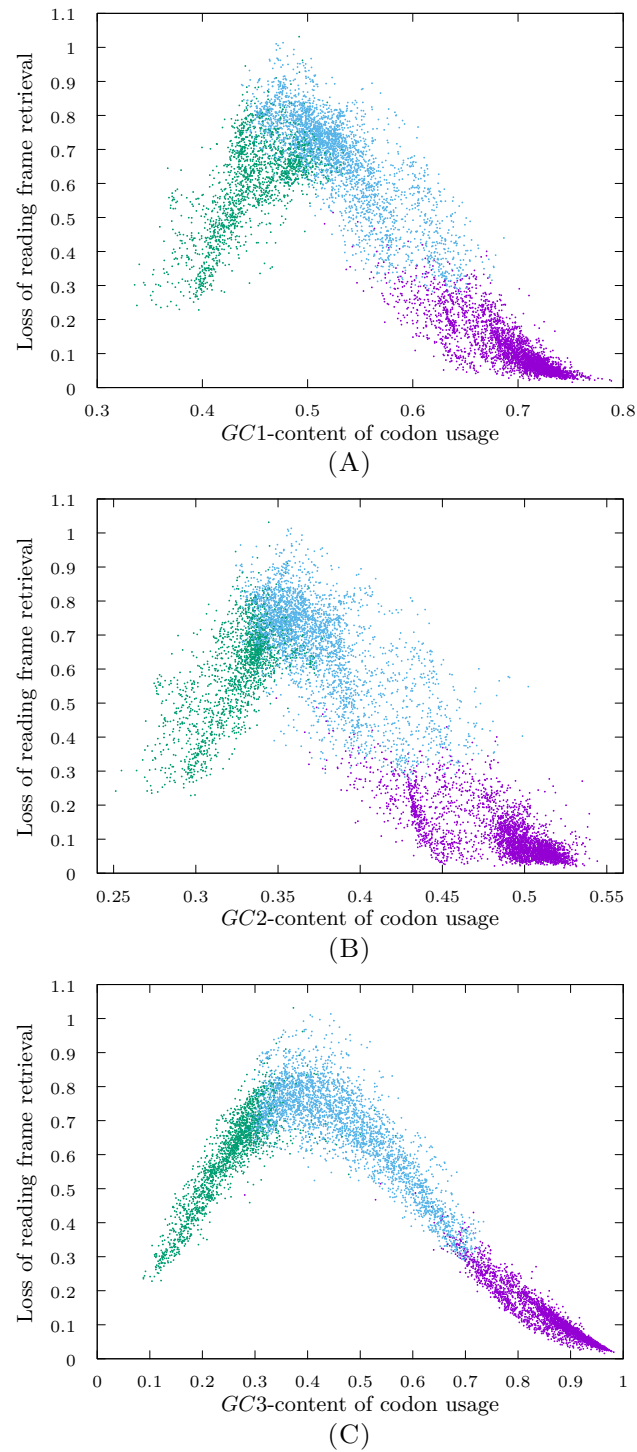


FIGURE 7. Genome galaxy of bacteria (8,345 genomes, 34,020,997 genes, 11,087,876,805 codons) with its center  $\mathcal{GC}$  (3.1) in blue, its upper arm  $\mathcal{GUA}$  (3.2) in green and its lower arm  $\mathcal{GLA}$  (3.3) in violet, identified by the  $GC$ -content in each of the 3 codon sites, and mainly by the  $GC3$ -content. Each point represents all the genes of a bacterial genome. The  $y$ -axis shows the reading frame retrieval function  $f$  (2.4). The  $x$ -axis shows the  $GC$ -content in the 3 codon sites: (A)  $GC1$ -content in the 1st codon site; (B)  $GC2$ -content in the 2nd codon site; (C)  $GC3$ -content in the 3rd codon site.

(3) for every  $i \in \{n+1, \dots, 64\}$  we have  $\omega_i = 0$ .

In other words, and referring to Definition 2.19, we require that

$$n(\mathcal{W}) = n; \quad n_h(\mathcal{W}) \geq n_h; \quad \text{and} \quad p_m \leq p_m(\mathcal{W}) \leq \frac{1}{n} \leq p_M(\mathcal{W}) \leq p_M.$$

Another observation is that if  $p_m = \frac{1}{n}$ , then Conditions (2) and (3) totally determine a unique weighted trinucleotide code, having  $w_i = \frac{1}{n}$  for  $i \in \{1, \dots, n\}$  and  $\omega_i = 0$  for  $i \in \{n+1, \dots, 64\}$ . It is similar if  $p_M = \frac{1}{n}$ . We thus assume in the rest of this section that

$$p_m < \frac{1}{n} < p_M. \quad (4.1)$$

We are interested in determining the minimum value and the maximum value taken by the dispersion over all weighted trinucleotide codes satisfying Conditions (1)–(3). We derive closed formulæ for these — along with weighted trinucleotides code attaining them.

**Definition 4.1.** Given Conditions (1)–(3) above and assuming (4.1), we define the maximum dispersion  $d_M$  and the minimum dispersion  $d_m$  as follows:

$$d_M = d_M(n, n_h, p_m, p_M) = \sup \{d(\mathcal{W}) : \mathcal{W} = (\omega_1, \dots, \omega_{64}) \text{ satisfies (1)–(3)}\}; \quad (4.2)$$

and

$$d_m = d_m(n, n_h, p_m, p_M) = \inf \{d(\mathcal{W}) : \mathcal{W} = (\omega_1, \dots, \omega_{64}) \text{ satisfies (1)–(3)}\}. \quad (4.3)$$

The determination of the minimum dispersion  $d_m$  is quick. It shows in particular that the value of  $d_m(n, n_h, p_m, p_M)$  does not depend on  $n_h$ .

**PROPOSITION 4.2.** *Suppose that Conditions (1)–(3) as above and (4.1) are satisfied. Then*

$$d_m = 2 \left[ 1 - \frac{n}{64} \right]. \quad (4.4)$$

The proof of Proposition 4.2 is given in Appendix B.

The determination of the maximum dispersion  $d_M$  is slightly more technical. We have the following proposition.

**PROPOSITION 4.3.** *Suppose that Conditions (1)–(3) as above and (4.1) are satisfied. If*

$$n_h \cdot p_M + (n - n_h) \cdot p_m \geq 1, \quad (4.5)$$

then

$$d_M = \begin{cases} 2 \left[ \left( p_m - \frac{1}{64} \right) \cdot n_h + 1 - n \cdot p_m \right] & \text{if } p_m \leq \frac{1}{64}, \\ 2 \left[ 1 - \frac{n}{64} \right] & \text{if } p_m > \frac{1}{64}. \end{cases} \quad (4.6a)$$

$$\text{if } p_m > \frac{1}{64}. \quad (4.6b)$$

If (4.5) does not hold, then with

$$\varepsilon = 1 - (n_h p_M + (n - n_h) p_m) > 0, \quad t_0 = \left\lfloor \frac{\varepsilon}{1/n - p_m} \right\rfloor, \quad \text{and} \quad z_1 = \varepsilon - t_0 \cdot \left( \frac{1}{n} - p_m \right),$$

we have

$$d_M = \begin{cases} 2 \left[ \left( p_M - \frac{1}{64} \right) \cdot n_h + t_0 \left( \frac{1}{n} - \frac{1}{64} \right) \right] & \text{if } p_m + z_1 \leq \frac{1}{64}, \\ 2 \left[ \left( p_m - \frac{1}{64} \right) (n_h + t_0 + 1) + 1 - n \cdot p_m \right] & \text{if } p_m + z_1 > \frac{1}{64} \text{ and } p_m \leq \frac{1}{64}, \\ 2 \left[ 1 - \frac{n}{64} \right] & \text{if } p_m > \frac{1}{64}. \end{cases} \quad (4.7a)$$

$$\text{if } p_m + z_1 > \frac{1}{64} \text{ and } p_m \leq \frac{1}{64}, \quad (4.7b)$$

$$\text{if } p_m > \frac{1}{64}. \quad (4.7c)$$



The proof of Proposition 4.3 is given in Appendix C.

Instead of imposing only a lower bound on the number  $n_h$  of codons of high frequency, as Condition (2) does, one could rather impose the exact number of such codons. In this case, the optimal values given by Proposition 4.3 are not necessarily always attained by a weighted trinucleotide code anymore, but are still the supremum of the possible values, as we explain in Appendix D.

It is important to stress that this mathematical theory and its formulæ of dispersion, i.e. Equations (4.4), (4.6a)–(4.6b) and (4.7a)–(4.7c), can be easily extended to any weighted codes over a finite alphabet, e.g. the amino acid alphabet, by replacing  $1/64$  with the cardinality of the code.

**4.2. Properties of the genetic code.** In order to study the evolution of the bacterial genetic code and to apply the mathematical theory developed in Section 4.1, three parameters must be obtained from the bacterial codon usage (see Appendix Table 1): the minimum probability, which is  $p_m = 0.06\%$ , given by the codon of lowest occurrence, i.e. *TAG*; the maximum probability, which is  $p_M = 4.32\%$ , given by the codon of highest occurrence, i.e. *GCC*; and the number of codons with high frequency, i.e. with a probability greater than  $\frac{1}{64}$ , which is  $n_h = 25$ . Note that  $\frac{n_h}{n} = \frac{25}{64}$  since there are  $n = 64$  occurring codons in the bacterial codon usage. We start by studying the maximum dispersion of the current genetic code over 64 codons with respect to the frequency of its codon of maximum and minimum probabilities.

4.2.1. *Maximum dispersion of the current genetic code as a function of its codon of maximum probability.* Figure 8 gives the maximum dispersion  $d_M$  of the current genetic code with 64 codons as a function of its number  $n_h$  of codons with high frequency,  $n_h \in \{1, \dots, 64\}$ , i.e. codons  $x$  with a probability at least  $\frac{1}{n} = \frac{1}{64}$  ( $\omega(x) \geq \frac{1}{64}$ ). The minimum probability is  $p_m = 0.06\%$ , given by the codon of lowest occurrence in bacteria, i.e. *TAG* (see Appendix Table 1). We considered 3 different values for the maximum probability  $p_M$ :  $4.32\%$  associated with the codon of highest occurrence in bacteria, i.e. *GCC* (see Appendix Table 1) (curve with green circles) and 2 arbitrarily chosen surrounding values:  $3\%$  (curve with violet disks) and  $6\%$  (curve with blue stars). Interestingly, for any maximum probability  $p_M$  the maximum dispersion  $d_M$  increases to a maximum and then decreases to 0 at  $n_h = 64$ . The curves have a common decreasing slope of equation  $y = 1.9232 - 0.03005x$  (see Equation (4.6a), which does not involve  $p_M$ ), but different increasing slopes, and thus different maxima. The change occurs for  $n_h = \left\lfloor \frac{1-64p_m}{p_M-p_m} \right\rfloor$  (see Equation (4.5)), and the maximum is thus attained for  $n_h = \left\lfloor \frac{1-64p_m}{p_M-p_m} \right\rfloor$  or  $n_h = \left\lceil \frac{1-64p_m}{p_M-p_m} \right\rceil$ . From Appendix Table 1, the number of codons with high frequency is  $n_h = 25$ . The maximum dispersion at  $n_h = 25$  is  $d_M = 1.17$ . Very interestingly, this value  $d_M = 1.17$  is very close to the maximum  $d_M = 1.23$  at  $n_h = 23$  of the curve with  $p_M = 4.32\%$  that is associated with bacteria (see Figure 8). As a biological consequence, bacteria have optimised the number of codons with high frequency in order to have a maximum of dispersion, and thus a maximum capacity to retrieve the reading frame in genes.

4.2.2. *Maximum dispersion of the current genetic code as a function of its codon of minimum probability.* Figure 9 gives the maximum dispersion  $d_M$  of the current genetic code with 64 codons as a function of its number  $n_h$  of codons with high frequency. The maximum probability is  $p_M = 4.32\%$ , given by the codon of highest occurrence in bacteria, i.e. *GCC* (see Appendix Table 1). We considered 3 different values for the minimum probability  $p_m$ :  $0.06\%$  associated with the codon of lowest occurrence in bacteria, i.e. *TAG* (see Appendix Table 1) (curve with green circles) and 2 arbitrarily chosen surrounding values:  $0$  (curve with violet disks) and  $0.5\%$

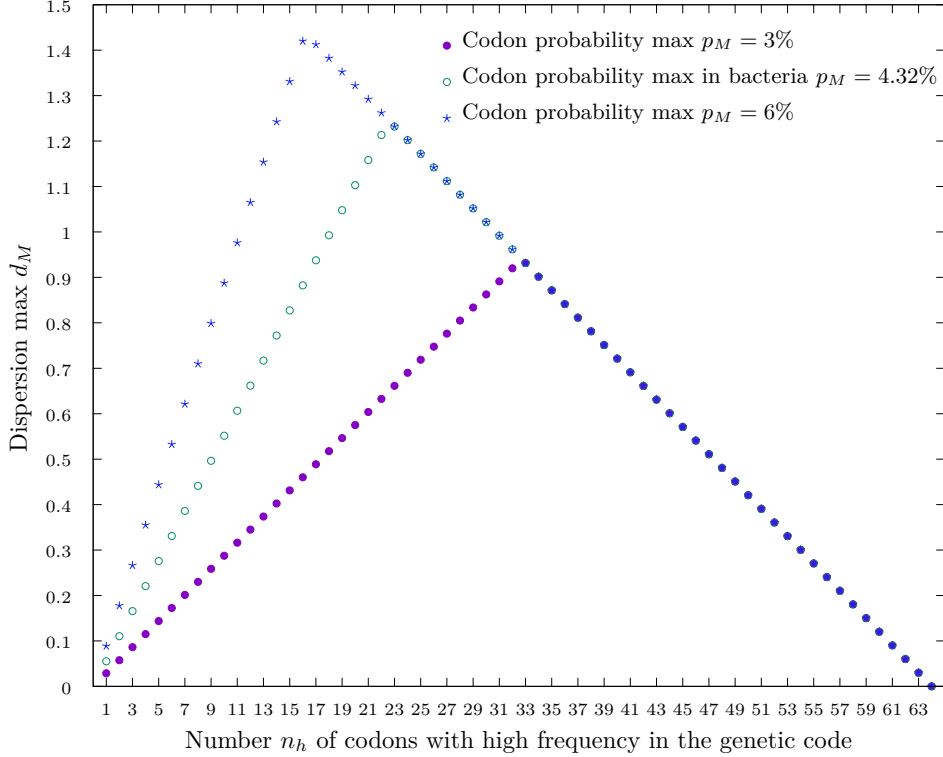


FIGURE 8. Maximum dispersion  $d_M$  of the current genetic code with 64 codons for three values of the codon of maximum probability  $p_M$ , the minimum probability  $p_m = 0.06\%$  being that of the codon *TAG* in bacteria (see Appendix Table 1). The  $x$ -axis shows the number  $n_h$  of codons with high frequency in the genetic code,  $n_h \in \{1, \dots, 64\}$ , i.e. codons  $x$  with a probability at least  $\frac{1}{64}$  ( $\omega(x) \geq \frac{1}{64}$ ). The  $y$ -axis shows the maximum dispersion  $d_M$  (see Proposition 4.3) of codon usage. Three curves corresponding to different values of the codon of maximum probability are displayed:  $p_M = 4.32\%$  associated with the codon *GCC* in bacteria (see Appendix Table 1) (curve with green circles) and 2 arbitrarily chosen surrounding values, namely  $p_M = 3\%$  (curve with violet disks) and  $p_M = 6\%$  (curve with blue stars).

(curve with blue stars). The value 0 is seen as a sort of limiting case for codons with very small frequencies, that is, when  $p_m(\mathcal{W})$  is a very small positive real. In theory, setting  $p_m = 0$  amounts to allowing the number of occurring codons to vary (case studied in Section 4.2.3), whereas we keep  $n = 64$  here. As in the previous case (Section 4.2.1), for any minimum probability  $p_m$  the maximum dispersion  $d_M$  increases to a maximum and then decreases to 0 at  $n_h = 64$ . However, the curves have a common increasing slope of equation  $y = 0.05515x$  (see Equation (4.7a)), but different decreasing slopes, and thus different maxima.

The curve with  $p_m = 0.06\%$  and  $p_M = 4.32\%$  is obviously identical in the two Sections 4.2.1 and 4.2.2 and the two Figures 8 and 9. Very interestingly, with  $p_M = 4.32\%$ , the curve with  $p_m = 0.06\%$  that is associated with bacteria is very close to the curve with  $p_m = 0$  giving the highest value for  $d_M$ . Indeed, at  $n_h = 25$  the maximum dispersion is equal to  $d_M = 1.17$  with  $p_m = 0.06\%$  and to  $d_M = 1.22$  with  $p_m = 0$ . As previously, bacteria have optimised the maximum dispersion, and thus a maximum capacity to retrieve the reading frame in genes.

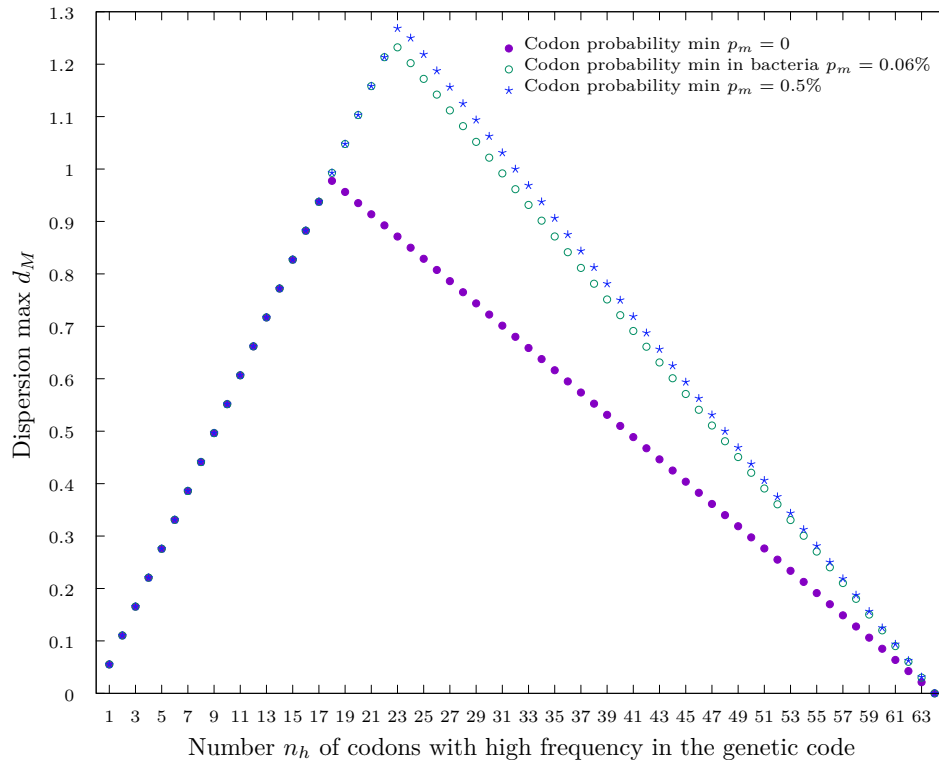


FIGURE 9. Maximum dispersion  $d_M$  of the current genetic code with 64 codons for three values of the minimum probability  $p_m$ , the maximum probability  $p_M = 4.32\%$  being that of the codon *GCC* in bacteria (see Appendix Table 1). The  $x$ -axis shows the number  $n_h$  of codons with high frequency in the genetic code,  $n_h \in \{1, \dots, 64\}$ , i.e. codons  $x$  with a probability at least  $\frac{1}{64}$  ( $\omega(x) \geq \frac{1}{64}$ ). The  $y$ -axis shows the maximum dispersion  $d_M$  (see Proposition 4.3) of codon usage. Three curves corresponding to different values of the codon of minimum probability are displayed:  $p_m = 0.06\%$  associated with the codon *TAG* in bacteria (see Appendix Table 1) (curve with green circles) and 2 arbitrarily chosen surrounding values, namely  $p_m = 0$  (curve with violet disks) and  $p_m = 0.5\%$  (curve with blue stars).

4.2.3. *Minimum and maximum dispersions of the evolutionary bacterial genetic code as a function of its number of codons.* Figure 10 gives the dispersion of the evolutionary bacterial genetic code as a function of its number  $n$  of codons,  $n \in \{1, \dots, 64\}$ , i.e. codons  $x$  with a probability  $\omega(x)$  greater than 0. Since  $n$  varies from 1 to 64, and we must have  $\frac{1}{n} \leq p_M$ , the parameter  $p_M$  cannot stay equal to its original value of 4.32% from the bacterial genome with 64 codons: we normalise it by setting  $p_M = \frac{4.32}{100} \cdot \frac{64}{n}$ . It then seems natural to similarly scale the minimum probability  $p_m$  instead of keeping it at the bacterial value 0.06%, and we do so by setting  $p_m = \frac{0.06}{100} \cdot \frac{n}{64}$ . Analogously, we make the parameter  $n_h$  vary with  $n$ , keeping the ratio  $\frac{n_h}{n}$  as close as possible to the bacterial value  $\frac{25}{64} \approx 0.39$ . Formally, we set  $n_h$  in  $\{1, \dots, n\}$  to be either  $\lfloor \frac{25n}{64} \rfloor$  or  $\lceil \frac{25n}{64} \rceil$ , depending on which value is closer to  $\frac{25n}{64}$  (and discarding the value 0, i.e., setting  $n_h = 1$  when  $n = 1$ , since as reported earlier we can always assume that  $n_h \geq 1$ ). The dispersion function  $d$  (2.1) of codon usage ranges in the interval  $[0, \frac{63}{32}] \approx [0, 1.97]$  (Proposition 2.8). The minimum dispersion  $d_m$  (curve with violet disks in Figure 10) has the maximum value  $\frac{63}{32} \approx 1.97$  at  $n = 1$  and the minimum value 0 at  $n = 64$ . It decreases along the straight line with equation  $y = 2 - \frac{x}{32}$  (see Equation (4.4)). The maximum dispersion  $d_M$  (curve with

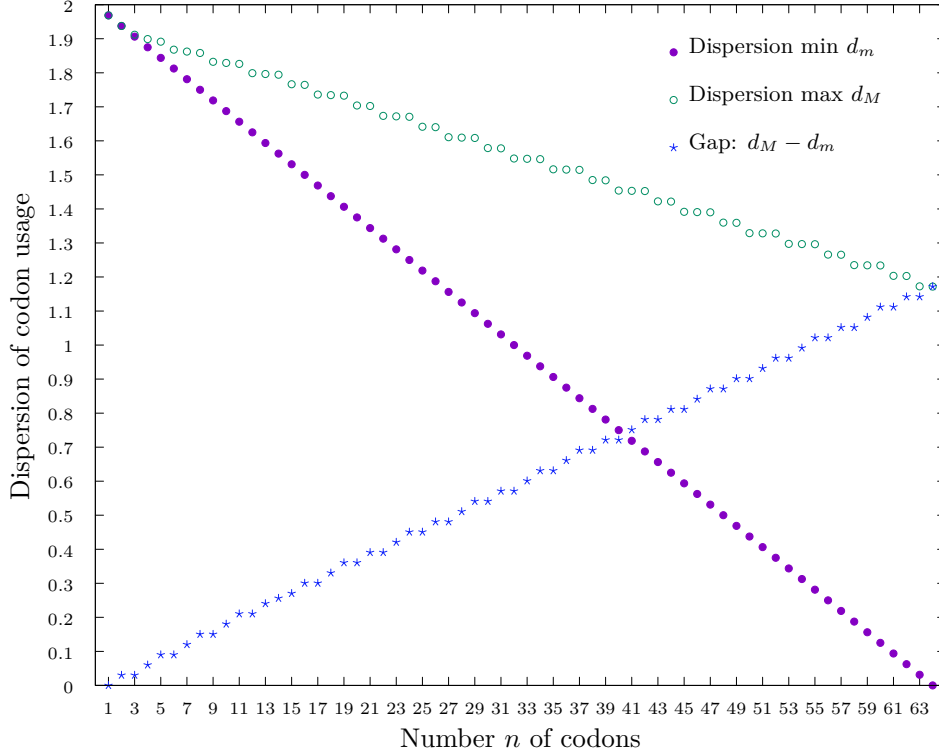


FIGURE 10. Dispersion of the evolutionary bacterial genetic code. From the bacterial codon usage (Appendix Table 1), three parameters are used: the (normalised) minimum probability is  $p_m = 0.06 \cdot \frac{64}{n}\%$ , based on the frequency of the codon of lowest occurrence in the bacterial genome, i.e. *TAG*; the (normalised) maximum probability is  $p_M = 4.32 \cdot \frac{64}{n}\%$ , based on the frequency of the codon of highest occurrence, i.e. *GCC*; and the (normalised) number  $n_h$  of codons with high frequency, i.e. with a probability at least  $\frac{1}{64}$ , defined as the positive integer that is closest to  $25 \cdot \frac{n}{64}$ . The  $x$ -axis shows the number  $n$  of codons in the genetic code,  $n \in \{1, \dots, 64\}$ , i.e. the codons  $x$  with a probability greater than 0 ( $\omega(x) > 0$ ). The  $y$ -axis shows the dispersion function  $d$  (2.1) of codon usage in the range  $[0, \frac{63}{32}] \approx [0, 1.97]$  (Proposition 2.8): the curve with violet disks is the minimum dispersion  $d_m$  (see Proposition 4.2), the curve with green circles is the maximum dispersion  $d_M$  (see Proposition 4.3) and the curve with blue stars is the dispersion difference  $\Delta = d_M - d_m$ .

green circles in Figure 10) has the maximum value  $\frac{63}{32} \approx 1.97$  at  $n = 1$ , as  $d_m$ , and the minimum value 1.17195 at  $n = 64$ . It decreases with  $n$ , approximately along the straight line with equation  $y = 1.948 - 0.012x$  (see Equation (4.6a), recalling that the values of  $p_m$  and  $n_h$  vary with  $n$ ). Thus, the dispersion difference  $\Delta = d_M - d_m$  has the minimum value 0 at  $n = 1$  and the maximum value 1.17195 at  $n = 64$ .


From a biological point of view, this theoretical result quantifies and explains that the more codons a code contains, the greater the dispersion and the greater the capacity of genes to retrieve the reading frame, or equivalently the lower the loss of reading frame retrieval (see the RFR function  $f$  (2.4) in Figure 1).

## 5. Conclusion

The reading frame retrieval (RFR) function  $f$  of genes expressed as a function of the codon usage dispersion  $d$  (from the uniform codon distribution  $1/64$ ), identifies a genome galaxy in bacteria (Figure 1). A simple probabilistic model for ambiguous sequences shows that the RFR function is a measure of the gene reading frame retrieval. Indeed, the RFR function increases with the ratio of ambiguous sequences and the ratio of ambiguous sequences decreases when the codon usage dispersion increases. This genome galaxy is studied by expressing the RFR function  $f$  according to the  $YZ$ -content ( $GC$ -,  $AG$ - and  $GT$ -content) of codon in bacteria (Figure 4). The classical  $GC$ -content is the best parameter for characterizing the upper arm, which is related to genomes with a low  $GC$ -content, and the lower arm, which is related to genomes with a high  $GC$ -content. The galaxy center has a  $GC$ -content around 0.5 (Figure 4A). Then, these results are confirmed by expressing the  $GC$ -content of codon as a function of the codon usage dispersion (Figure 5A). Finally, the bacterial genome galaxy is better described with the  $GC3$ -content in the 3rd codon site compared to the  $GC1$ -content and  $GC2$ -content in the 1st and 2nd codons sites, respectively (Figure 7C).

Whereas the codon usage is used extensively by biologists, its dispersion is surprisingly little known and unused, even though it is a classical parameter in basic statistics. With this in mind, and also to study the genome galaxy, we have developed here a mathematical theory of codon usage dispersion by deriving several formulæ. It shows three important parameters that should be considered by biologists: the codon of highest frequency (i.e. the parameter  $p_M$ ), the codon of lowest frequency (i.e. the parameter  $p_m$ ) and the number of codons with high frequency, i.e. greater than  $100/64 = 1.5625\%$  (i.e. the parameter  $n_h$ ). The derived formulæ of dispersion can be easily extended to any weighted codes over a finite alphabet, e.g. the amino acid alphabet. The theory developed shows that bacteria have optimised the codon dispersion to be maximal, and thus a maximum capacity to retrieve the reading frame in genes, in two ways: (i) the existence of stop codons with frequencies  $p_m \approx 0$ , e.g. the bacterial codon  $TAG$  of lowest frequency  $p_m = 0.06\%$  (Figure 9); (ii) the number  $n_h$  of codons with high frequency, e.g.  $n_h = 25$  is almost optimal with the bacterial codon  $GCC$  of highest occurrence  $p_M = 4.32\%$  (Figure 8).

*Disclosure of interest:* The authors report no conflict of interest.

 The authors have applied a CREATIVE COMMONS ATTRIBUTION 4.0 INTERNATIONAL LICENSE to any Author Accepted version arising from this submission.  
<http://creativecommons.org/licenses/by/4.0/>

### Appendix A. Codon usage of bacterial kingdom

TABLE 1. Codon usage of 34,020,997 genes of 8345 bacterial genomes (11,087,876,805 codons) obtained from the codon statistics database (CSD) [26].

<i>AAA</i>	2.37	<i>CAA</i>	1.20	<i>GAA</i>	2.91	<i>TAA</i>	0.12
<i>AAC</i>	1.80	<i>CAC</i>	1.27	<i>GAC</i>	3.42	<i>TAC</i>	1.56
<i>AAG</i>	2.00	<i>CAG</i>	2.16	<i>GAG</i>	3.22	<i>TAG</i>	0.06
<i>AAT</i>	1.64	<i>CAT</i>	0.78	<i>GAT</i>	2.25	<i>TAT</i>	1.35
<i>ACA</i>	0.93	<i>CCA</i>	0.63	<i>GCA</i>	1.43	<i>TCA</i>	0.64
<i>ACC</i>	2.56	<i>CCC</i>	1.39	<i>GCC</i>	4.32	<i>TCC</i>	1.25
<i>ACG</i>	1.51	<i>CCG</i>	2.14	<i>GCG</i>	3.22	<i>TCG</i>	1.23
<i>ACT</i>	0.76	<i>CCT</i>	0.67	<i>GCT</i>	1.30	<i>TCT</i>	0.67
<i>AGA</i>	0.54	<i>CGA</i>	0.43	<i>GGA</i>	1.39	<i>TGA</i>	0.15
<i>AGC</i>	1.28	<i>CGC</i>	2.26	<i>GGC</i>	3.63	<i>TGC</i>	0.53
<i>AGG</i>	0.38	<i>CGG</i>	1.64	<i>GGG</i>	1.43	<i>TGG</i>	1.31
<i>AGT</i>	0.69	<i>CGT</i>	0.80	<i>GGT</i>	1.54	<i>TGT</i>	0.29
<i>ATA</i>	0.82	<i>CTA</i>	0.45	<i>GTA</i>	1.05	<i>TTA</i>	1.25
<i>ATC</i>	2.76	<i>CTC</i>	2.23	<i>GTC</i>	2.66	<i>TTC</i>	2.11
<i>ATG</i>	2.15	<i>CTG</i>	3.86	<i>GTG</i>	2.66	<i>TTG</i>	1.21
<i>ATT</i>	1.91	<i>CTT</i>	1.01	<i>GTT</i>	1.20	<i>TTT</i>	1.61

## Appendix B. Proof of Proposition 4.2

We start by defining a weighted trinucleotide code  $\mathcal{W} = (\omega_1, \dots, \omega_{64})$  that satisfies Conditions (1)–(3) by setting  $\omega_i = \frac{1}{n}$  if  $1 \leq i \leq n$ , and  $\omega_i = 0$  if  $n_h + 1 \leq i \leq 64$ . Then  $\mathcal{W}$  readily satisfies Conditions (1)–(3). Moreover,  $d(\mathcal{W}) = 2 - \frac{n}{32}$ . Indeed, if  $i \in \{1, \dots, n\}$  then  $\omega_i = \frac{1}{n} \geq \frac{1}{64}$ , so  $\sum_{i=1}^n \left| \omega_i - \frac{1}{64} \right| = 1 - \frac{n}{64}$ ; moreover if  $i \in \{n+1, \dots, 64\}$  then  $\omega_i = 0$  so  $\sum_{i=n+1}^{64} \left| \omega_i - \frac{1}{64} \right| = \frac{64-n}{64} = 1 - \frac{n}{64}$ .

It remains to show that if a weighted trinucleotide code  $\mathcal{W}' = (\omega'_1, \dots, \omega'_{64})$  satisfies Conditions (1)–(3), then  $d(\mathcal{W}') \geq d(\mathcal{W})$ . First, note that if  $n = 64$ , then  $d(\mathcal{W}) = 0$ , which is trivially minimum. So we now assume that  $n \leq 63$ , and we proceed as follows. Since the function  $d_m$  is the minimization of a convex function over a convex domain, it suffices to prove that  $d(\mathcal{W})$  is a local minimum, that is, if a weighted trinucleotide code  $\mathcal{W}'$  still satisfying Conditions (1)–(3) is produced by small enough modifications of the values  $\omega_1, \dots, \omega_{64}$ , then  $d(\mathcal{W}') \geq d(\mathcal{W}) = 2 - \frac{n}{32}$ . Fix  $\varepsilon > 0$  small enough that  $\frac{1}{64} + \varepsilon < \frac{1}{n}$ , which is possible since  $n \leq 63$  by our assumption. Now, if  $|\omega'_i - \omega_i| \leq \varepsilon$  for  $i \in \{1, \dots, 64\}$ , then since  $\mathcal{W}'$  satisfies Condition (1) we have  $\omega'_i \geq \omega_i = \frac{1}{n} > \frac{1}{64}$  if  $1 \leq i \leq n_h$ , and  $\omega'_i \geq \omega_i - \varepsilon = \frac{1}{n} - \varepsilon > \frac{1}{64}$  if  $n_h + 1 \leq i \leq n$ . So  $\left| \omega'_i - \frac{1}{64} \right| = \omega'_i - \frac{1}{64}$  for  $i \in \{1, \dots, n\}$ . Consequently,

$$\sum_{i=1}^n \left| \omega'_i - \frac{1}{64} \right| = \sum_{i=1}^n \left( \omega'_i - \frac{1}{n} \right) + \sum_{i=1}^n \left( \frac{1}{n} - \frac{1}{64} \right). \quad (\text{B.1})$$

As a result, using that  $\omega'_i = 0 = \omega_i$  if  $n+1 \leq i \leq 64$  since  $\mathcal{W}'$  must satisfy Condition (3), we infer from (B.1) that

$$\begin{aligned} d(\mathcal{W}') &= \sum_{i=1}^n \left( \omega'_i - \frac{1}{n} \right) + d(\mathcal{W}) \\ &= d(\mathcal{W}) - 1 + \sum_{i=1}^n \omega'_i \\ &= d(\mathcal{W}). \end{aligned}$$

This concludes the proof. □



### Appendix C. Proof of Proposition 4.3

Suppose first that (4.5) holds. Let  $z_0 = \frac{1-n \cdot p_m}{n_h}$ , and note that  $z_0 \geq 0$  by (4.1). We set

$$\forall i \in \{1, \dots, 64\}, \quad \omega_i = \begin{cases} p_m + z_0 & \text{if } 1 \leq i \leq n_h, \\ p_m & \text{if } n_h + 1 \leq i \leq n, \\ 0 & \text{otherwise.} \end{cases}$$

Then  $\mathcal{W} = (\omega_1, \dots, \omega_{64})$  defines a weighted trinucleotide code, since it consists of non-negative real numbers summing to 1. This code  $\mathcal{W}$  does satisfy the required properties. The only condition that could be violated is (1). However,  $\frac{(n-n_h)p_m}{n_h} \geq \frac{1}{n_h} - p_m$  by (4.5), so  $p_m + z_0 = \frac{1-(n-n_h)p_m}{n_h} \leq p_m$  on the one hand, and  $\frac{(n-n_h)p_m}{n_h} \leq \frac{1}{n_h} - \frac{1}{n}$  by (4.1) so  $p_m + z_0 \geq \frac{1}{n}$  on the other hand. Consequently,  $d_M \geq d(\mathcal{W})$ . Moreover,  $d(\mathcal{W})$  is equal to the right side of (4.6a) if  $p_m \leq \frac{1}{64}$ , and to the right side of (4.6b) otherwise. To see this, we define  $d_1 = \sum_{i=1}^{n_h} \left| \omega_i - \frac{1}{64} \right|$  and  $d_2 = \sum_{i=n_h+1}^n \left| \omega_i - \frac{1}{64} \right|$ . If  $i \in \{1, \dots, n_h\}$ , then  $\omega_i = p_m + z_0 \geq \frac{1}{n} \geq \frac{1}{64}$  so

$$d_1 = n_h \cdot \left( p_m + z_0 - \frac{1}{64} \right) = 1 - (n - n_h) \cdot p_m - \frac{n_h}{64} = 1 + n_h \cdot \left( p_m - \frac{1}{64} \right) - n \cdot p_m; \quad (\text{C.1})$$

while if  $i \in \{n_h + 1, \dots, n\}$ , then  $\omega_i = p_m$ , so if  $p_m \leq \frac{1}{64}$ ,

$$d_2 = (n - n_h) \cdot \left( \frac{1}{64} - p_m \right) = \frac{n}{64} + n_h \cdot \left( p_m - \frac{1}{64} \right) - n \cdot p_m, \quad (\text{C.2})$$

and if  $p_m > \frac{1}{64}$ ,

$$d_2 = (n - n_h) \cdot \left( p_m - \frac{1}{64} \right) = -\frac{n}{64} - n_h \cdot \left( p_m - \frac{1}{64} \right) + n \cdot p_m; \quad (\text{C.3})$$

finally, if  $i \in \{n + 1, \dots, 64\}$ , then  $\omega_i = 0$  and hence  $\sum_{i=n+1}^{64} \left| \omega_i - \frac{1}{64} \right| = 1 - \frac{n}{64}$ . Summing this with (C.1) and either (C.2) or (C.3) yields (4.6a) or (4.6b), respectively.

It remains to prove that if a weighted trinucleotide code  $\mathcal{W}' = (\omega'_1, \dots, \omega'_{64})$  satisfies Conditions (1)–(3), then  $d(\mathcal{W}') \leq d(\mathcal{W})$ . By Condition (3), it suffices to prove that  $\sum_{i=1}^n \left| \frac{1}{64} - \omega'_i \right| \leq \sum_{i=1}^n \left| \frac{1}{64} - \omega_i \right|$ . For convenience we set  $S_1 = \sum_{i=1}^{n_h} \omega_i$  and  $S_2 = \sum_{i=n_h+1}^n \omega_i$ . We similarly define  $S'_1, S'_2$  as well as  $d'_1$  and  $d'_2$  with respect to  $\mathcal{W}'$  instead of  $\mathcal{W}$ . Our goal is thus to show that  $d'_1 + d'_2 \leq d_1 + d_2$ . Note that  $S_1 + S_2 = 1 = S'_1 + S'_2$ .

As  $\omega'_i \geq \frac{1}{64}$  for  $i \in \{1, \dots, n_h\}$ , we deduce that  $d'_1 = S'_1 - \frac{n_h}{64} = 1 - S'_2 - \frac{n_h}{64}$ , and hence (C.1) implies that  $d'_1 - d_1 = (n - n_h) \cdot p_m - S'_2$ .

To express  $d'_2$ , let

$$I_2^+ = \left\{ i \in \{n_h + 1, \dots, n\} : \omega'_i > \frac{1}{64} \right\},$$

and  $I_2^- = \{n_h + 1, \dots, n\} \setminus I_2^+$ , thus  $|I_2^+| = (n - n_h) - |I_2^-|$  and  $\sum_{i \in I_2^+} \omega'_i = S'_2 - \sum_{i \in I_2^-} \omega'_i$ . Consequently,

$$\begin{aligned}
d'_2 &= \sum_{i=n_h+1}^n \left| \omega'_i - \frac{1}{64} \right| = \sum_{i \in I_2^+} \left( \omega'_i - \frac{1}{64} \right) + \sum_{i \in I_2^-} \left( \frac{1}{64} - \omega'_i \right) \\
&= -\frac{1}{64} \cdot \left( |I_2^+| - |I_2^-| \right) + \sum_{i \in I_2^+} \omega'_i - \sum_{i \in I_2^-} \omega'_i \\
&= -\frac{1}{64} \cdot \left( (n - n_h) - 2|I_2^-| \right) + S'_2 - 2 \sum_{i \in I_2^-} \omega'_i \\
&\leq -\frac{1}{64} \cdot \left( (n - n_h) - 2|I_2^-| \right) + S'_2 - 2 \sum_{i \in I_2^-} p_m \\
&= 2|I_2^-| \left( \frac{1}{64} - p_m \right) + S'_2 - \frac{n - n_h}{64},
\end{aligned}$$

where the inequality holds because  $\omega'_i \geq p_m$  for each  $i \in I_2^-$ . Furthermore, if  $p_m > \frac{1}{64}$ , then  $d_2 = (n - n_h) \cdot (p_m - \frac{1}{64})$ , and hence

$$\begin{aligned}
d'_1 + d'_2 - (d_1 + d_2) &= d'_1 - d_1 + d'_2 - d_2 \\
&= 2|I_2^-| \left( \frac{1}{64} - p_m \right) \leq 0,
\end{aligned}$$

since  $p_m > \frac{1}{64}$ .

Finally, if  $p_m \leq \frac{1}{64}$ , then  $d_2 = (n - n_h) \cdot (\frac{1}{64} - p_m)$ , and therefore,

$$\begin{aligned}
d'_1 + d'_2 - (d_1 + d_2) &= d'_1 - d_1 + d'_2 - d_2 \\
&\leq 2(n - n_h) \cdot \left( p_m - \frac{1}{64} \right) + 2|I_2^-| \cdot \left( \frac{1}{64} - p_m \right) \\
&= 2 \left( p_m - \frac{1}{64} \right) \cdot \left( (n - n_h) - |I_2^-| \right).
\end{aligned}$$

It follows that  $d'_1 + d'_2 \leq d_1 + d_2$ , because  $p_m - \frac{1}{64} \leq 0$  on the one hand, and  $(n - n_h) - |I_2^-| \geq 0$  on the other hand since  $I_2^-$  is a subset of  $\{n_h + 1, \dots, n\}$ .

**Suppose now that (4.5) does not hold, so**

$$n_h \cdot p_M + (n - n_h) \cdot p_m < 1. \quad (\text{C.4})$$

This implies that  $p_m < \frac{1}{n}$ . As in the statement of the proposition, we set  $\varepsilon = 1 - (n_h \cdot p_M + (n - n_h) \cdot p_m)$  and  $t = \frac{\varepsilon}{1/n - p_m}$ , so  $\varepsilon$  and  $t$  are positive; and we also set  $t_0 = \lfloor t \rfloor$  and  $z_1 = \varepsilon - t_0 \cdot (\frac{1}{n} - p_m)$ , so  $z_1 \geq 0$ . We note that  $n_h + t_0 + 1 \leq n$ , for otherwise we infer that  $\frac{1}{n} \geq p_M$ , contrary to (4.1). Indeed, if  $n_h + t_0 \geq n$ , then  $n_h + t \geq n$ , that is,

$$n_h + \frac{1 - n_h p_M - n p_m + n_h p_m}{\frac{1}{n} - p_m} \geq n$$

so

$$\frac{n_h}{n} - n_h p_m + 1 - n_h p_M - n p_m + n_h p_m \geq 1 - n p_m,$$

which yields that  $\frac{n_h}{n} - n_h p_M \geq 0$  and hence  $\frac{1}{n} \geq p_M$  since  $n_h > 0$ .

Then setting

$$\forall i \in \{1, \dots, 64\}, \quad \omega_i = \begin{cases} p_M & \text{if } 1 \leq i \leq n_h, \\ \frac{1}{n} & \text{if } n_h + 1 \leq i \leq n_h + t_0, \\ p_m + z_1 & \text{if } i = n_h + t_0 + 1, \\ p_m & \text{if } n_h + t_0 + 2 \leq i \leq n, \\ 0 & \text{otherwise,} \end{cases}$$

defines a weighted trinucleotide code, since the sequence  $\mathcal{W} = (\omega_1, \dots, \omega_{64})$  consists of non-negative real numbers summing to 1. Conditions (1)–(3) can be violated only if  $p_m + z_1 > \frac{1}{n}$ . However, since  $t_0 = \lfloor t \rfloor > t - 1$ ,

$$p_m + z_1 = p_m + \varepsilon - t_0 \left( \frac{1}{n} - p_m \right) < \varepsilon - t \left( \frac{1}{n} - p_m \right) + \frac{1}{n} = \frac{1}{n}. \quad (\text{C.5})$$

Moreover, if  $p_m \leq \frac{1}{64}$  then  $d(\mathcal{W})$  equals the right side of (4.7a) or of (4.7b), depending on whether  $p_m + z_1 \leq \frac{1}{64}$  or not, while if  $p_m > \frac{1}{64}$  then  $d(\mathcal{W})$  equals the right side of (4.7c). This follows from the definitions by a direct computation, recalling that  $n_h p_M = 1 - (n - n_h) p_m - \varepsilon$ . Indeed, if  $i \in \{1, \dots, n_h + t_0\}$  then  $\left| \omega_i - \frac{1}{64} \right| = \omega_i - \frac{1}{64}$  and hence

$$\sum_{i=1}^{n_h+t_0} \left| \omega_i - \frac{1}{64} \right| = \left( p_M - \frac{1}{64} \right) \cdot n_h + \left( \frac{1}{n} - \frac{1}{64} \right) \cdot t_0. \quad (\text{C.6})$$

If  $p_m \leq \frac{1}{64}$ , then for  $i \in \{n_h + t_0 + 2, \dots, 64\}$  we have  $\left| \omega_i - \frac{1}{64} \right| = \frac{1}{64} - \omega_i$ , and hence

$$\sum_{i=n_h+t_0+2}^{64} \left| \omega_i - \frac{1}{64} \right| = (n_h + t_0 + 1 - n) \left( p_m - \frac{1}{64} \right) + 1 - \frac{n}{64}, \quad (\text{C.7})$$

while if  $p_m > \frac{1}{64}$ , then  $\left| \omega_i - \frac{1}{64} \right| = p_m - \frac{1}{64}$  for  $i \in \{n_h + t_0 + 2, \dots, n\}$ , and  $\left| \omega_i - \frac{1}{64} \right| = \frac{1}{64}$  for  $i \in \{n + 1, \dots, 64\}$ , so that

$$\sum_{i=n_h+t_0+2}^{64} \left| \omega_i - \frac{1}{64} \right| = (n_h + t_0 + 1 - n) \left( \frac{1}{64} - p_m \right) + 1 - \frac{n}{64}. \quad (\text{C.8})$$

Now if  $p_m + z_1 > \frac{1}{64}$  then

$$\left| \omega_{n_h+t_0+1} - \frac{1}{64} \right| = (n_h + t_0 + 1 - n) \cdot p_m - n_h \cdot p_M - \frac{t_0}{n} + 1 - \frac{1}{64}, \quad (\text{C.9})$$

so the sum of (C.6), (C.7) and (C.9) shows that  $d(\mathcal{W})$  equals the right side of (4.7b) if  $p_m \leq \frac{1}{64}$ , while the sum of (C.6), (C.8) and (C.9) shows that  $d(\mathcal{W})$  equals the right side of (4.7c) if  $p_m > \frac{1}{64}$ . Moreover, if on the contrary  $p_m + z_1 \leq \frac{1}{64}$ , and in particular  $p_m \leq \frac{1}{64}$  as  $z_1 \geq 0$ , then

$$\left| \omega_{n_h+t_0+1} - \frac{1}{64} \right| = -(n_h + t_0 + 1 - n) \cdot p_m + n_h \cdot p_M + \frac{t_0}{n} - 1 + \frac{1}{64}, \quad (\text{C.10})$$

so the sum of (C.6), (C.7) and (C.10) shows that  $d(\mathcal{W})$  equals the right side of (4.7a).

We now prove that  $\mathcal{W}$  has the largest dispersion among all weighted trinucleotide codes satisfying Conditions (1)–(3). To this end, let  $\mathcal{W}' = (\omega'_1, \dots, \omega'_{64})$  be such a code, that moreover maximises the dispersion over all weighted trinucleotide codes satisfying Conditions (1)–(3).

We first show that we can assume that  $\omega'_i = p_M$  for each  $i \in \{1, \dots, n_h\}$ . Indeed, suppose that there exists  $i \in \{1, \dots, n_h\}$  such that  $\omega'_i = p_M - \delta$  for some positive real  $\delta$ . Because  $\omega'_k \leq p_M = \omega_k$  for any  $k \in \{1, \dots, n_h\}$  and  $\sum_{i=1}^n \omega'_i = 1 = \sum_{i=1}^n \omega_i$ , we infer the existence of a set  $J \subseteq \{n_h + 1, \dots, n\}$  such that

- $\sum_{j \in J} \omega'_j \geq \delta + \sum_{j \in J} \omega_j$ ; and

- $\omega'_j > \omega_j$  for each  $j \in J$ .

Since  $p_m \leq \omega_j < \omega'_j \leq \frac{1}{n}$  for  $j \in J$ , we can define a weighted trinucleotide code  $\mathcal{Z} = (\zeta_1, \dots, \zeta_{64})$  satisfying Conditions (1)–(3) by setting  $\zeta_i = p_M$ , next  $\zeta_k = \omega'_k$  if  $k \notin J \cup \{i\}$ , and finally defining  $\zeta_j$  for  $j \in J$  such that  $\zeta_j \leq \omega'_j$  and  $\sum_{j \in J} \zeta_j = (\sum_{j \in J} \omega'_j) - \delta$ . Now,  $\sum_{k \notin J} \left| \zeta_k - \frac{1}{64} \right| = \delta + \sum_{k \notin J} \left| \omega'_k - \frac{1}{64} \right|$  and  $\sum_{j \in J} \left| \zeta_j - \frac{1}{64} \right| \geq -\delta + \sum_{j \in J} \left| \omega'_j - \frac{1}{64} \right|$ , so that  $d(\mathcal{Z})$  is at least, and hence equal to,  $d(\mathcal{W}')$ . Consequently, we can now assume that  $\omega'_i = p_M$  for  $i \in \{1, \dots, n_h\}$ .

We similarly show that we can assume that  $\omega'_i = \frac{1}{n}$  if  $n_h + 1 \leq i \leq n_h + t_0$ . Indeed, suppose that there exists  $i \in \{n_h + 1, \dots, n_h + t_0\}$  such that  $\omega'_i = \frac{1}{n} - \delta$  for some positive real  $\delta$ . Because  $\omega'_k \leq \frac{1}{n} = \omega_k$  for  $k \in \{n_h + 1, \dots, n_h + t_0\}$ , and  $\omega'_k = p_M = \omega_k$  if  $1 \leq k \leq n_h$ , we infer the existence of a set  $J \subseteq \{n_h + t_0 + 1, \dots, n\}$  such that

- $\sum_{j \in J} \omega'_j \geq \delta + \sum_{j \in J} \omega_j$ ; and
- $\omega'_j > \omega_j$  for each  $j \in J$ .

As before, we can then define a weighted trinucleotide code  $\mathcal{Z} = (\zeta_1, \dots, \zeta_{64})$  satisfying Conditions (1)–(3) and with dispersion at least  $d(\mathcal{W}')$  by setting  $\zeta_i = \frac{1}{n}$ , next  $\zeta_k = \omega'_k$  if  $k \notin J \cup \{i\}$ , and finally defining  $\zeta_j$  for  $j \in J$  such that  $\zeta_j \leq \omega'_j$  and  $\sum_{j \in J} \zeta_j = (\sum_{j \in J} \omega'_j) - \delta$ . In total, we can thus assume that  $\omega'_i = \omega_i$  if  $1 \leq i \leq n_h + t_0$ .

We now conclude that  $d(\mathcal{W}') = d(\mathcal{W})$ . This is true if  $\omega'_k = \omega_k$  for  $k \in \{n_h + t_0 + 2, \dots, n\}$ , since then  $\mathcal{W}$  and  $\mathcal{W}'$  must be equal as both sum to 1. Recalling that  $\omega'_k \geq p_m = \omega_k$  for each  $k \in \{n_h + t_0 + 2, \dots, n\}$ , we can thus suppose that  $\sum_{j=n_h+t_0+2}^n \omega'_j = \delta + \sum_{j=n_h+t_0+2}^n \omega_k$  for some positive real  $\delta$ . Because, in addition  $\omega'_k = \omega_k$  if  $1 \leq k \leq n_h + t_0$ , we infer that  $\omega'_{n_h+t_0+1} = \omega_{n_h+t_0+1} - \delta$ . Therefore,  $d(\mathcal{W}')$  is most, and hence equal to,  $d(\mathcal{W})$ . We have proved that  $\mathcal{W}$  indeed has the largest dispersion among all weighted trinucleotide codes satisfying Conditions (1)–(3). This concludes the proof.  $\square$

### Appendix D. Case with a given number of codons of high frequency

One could want to insist that the number of codons of high frequency is precisely  $n_h$  rather than at least  $n_h$ , thereby replacing Condition (2) from Section 4.1, namely

$$(2) \text{ for every } i \in \{n_h + 1, \dots, n\}, \text{ we have } p_m \leq \omega_i \leq \frac{1}{n},$$

by the following condition

$$(2') \text{ for every } i \in \{n_h + 1, \dots, n\}, \text{ we have } p_m \leq \omega_i < \frac{1}{n}.$$

The extremal values proved in Propositions 4.2 and 4.3 are left unchanged under our assumption that  $p_m < \frac{1}{n} < p_M$  (for otherwise, as reported above, all  $n$  occurring codons must have frequency  $\frac{1}{n}$ ). This clearly holds for (4.6a) and (4.6b), since the weighted trinucleotide code provided in the proof already satisfies Condition (2'), as  $p_m < \frac{1}{n}$ .

The other weighted trinucleotide codes provided in the proofs of Propositions 4.2 and 4.3 can be slightly modified to satisfy Condition (2') instead of Condition (2), and have dispersion arbitrarily close to the original one. Indeed, for Proposition 4.2, we can choose  $\delta > 0$  such that  $f_m := \frac{1}{n} - \delta \geq p_m$  and  $f_M := \frac{1}{n} + \frac{n-n_h}{n_h}\delta \leq p_M$ . We then change the value of  $\omega_i$  to  $f_M$  if  $1 \leq i \leq n_h$ , and to  $f_m$  if  $n_h + 1 \leq i \leq n$ . Note that the total sum remains 1, as

$$(n - n_h)f_m + n_h f_M = \frac{n - n_h}{n} - (n - n_h)\delta + \frac{n_h}{n} + (n - n_h)\delta = 1.$$

Furthermore,  $\left|f_M - \frac{1}{64}\right| = \left|\frac{1}{n} - \frac{1}{64}\right| + \frac{n-n_h}{n_h}\delta$  and  $\left|f_m - \frac{1}{64}\right| \leq \left|\frac{1}{n} - \frac{1}{64}\right| + \delta$ . Therefore, the obtained weighted trinucleotide code has dispersion at most  $2 - \frac{n}{32} + 2(n - n_h)\delta$ , which can be made arbitrarily close to  $2 - \frac{n}{32}$  by choosing  $\delta$  arbitrarily close to 0 (and positive). As a side remark, if  $n \leq 63$  then  $\delta$  can also be chosen small enough that  $f_m \geq \frac{1}{64}$ , and then the dispersion of the newly defined weighted trinucleotide code is again exactly  $2 - \frac{n}{32}$ . Indeed, we have  $\left|f_m - \frac{1}{64}\right| = \left|\frac{1}{n} - \frac{1}{64}\right| - \delta$ , so that

$$(n - n_h) \left|f_m - \frac{1}{64}\right| + n_h \left|f_M - \frac{1}{64}\right| = (n - n_h) \left|\frac{1}{n} - \frac{1}{64}\right| + n_h \left|\frac{1}{n} - \frac{1}{64}\right|.$$

For the weighted trinucleotide code  $\mathcal{W} = (\omega_1, \dots, \omega_{64})$  provided to establish (4.7a)–(4.7c), first recall that  $p_m + z_1 < \frac{1}{n}$  by (C.5), and hence  $\mathcal{W}$  satisfies Condition (2') unless  $t_0 \geq 1$ , in which case the values  $\omega_{n_h+1}, \dots, \omega_{n_h+t_0}$  are all equal to  $\frac{1}{n}$ . As already observed in the proof of Proposition 4.3, it holds that  $n_h + t_0 \leq n - 1$ . We can choose  $\delta > 0$  such that  $f_m := \frac{1}{n} - \delta > p_m$  and  $p_m + z_1 + t_0\delta < \frac{1}{n}$ , recalling that  $p_m + z_1 < \frac{1}{n}$ . If  $p_m + z_1 < \frac{1}{64}$ , then up to further reducing the value of  $\delta$ , we can moreover suppose that  $p_m + z_1 + t_0\delta < \frac{1}{64}$ . We now change the value of  $\omega_i$  to  $f_m$  for  $i \in \{n_h + 1, \dots, n_h + t_0\}$ , and to  $p_m + z_1 + t_0\delta$  if  $i = n_h + t_0 + 1$ . We note that the obtained code satisfies Condition (2') as well as Conditions (1) and (3), and one sees similarly as before that its dispersion differs from that of the original code by at most  $2t_0\delta$ , which can be made arbitrarily close to 0 by choosing  $\delta$  arbitrarily close to 0 (and positive). As a side remark, if  $p_m + z_1 \geq \frac{1}{64}$ , then the dispersion of the newly defined code remains unchanged, thus attaining the right side of (4.7b).

## References

- [1] D. G. Arquès and C. J. Michel, *A complementary circular code in the protein coding genes*, Journal of Theoretical Biology **182** (1996), 45–58.
- [2] V. Bali and Z. Bebok, *Decoding mechanisms by which silent codon changes influence protein biogenesis and function*, International Journal of Biochemistry and Cell Biology **64** (2015), 58–74.
- [3] F. Buhr, S. Jha, M. Thommen, J. Mittelstaet, F. Kutz, H. Schwalbe, M. Rodnina, and A. A. Komar, *Synonymous codons direct cotranslational folding toward different protein conformations*, Molecular Cell **61** (2016), 341–351.
- [4] G. Dila, R. Ripp, C. Mayer, O. Poch, C. J. Michel, and J. D. Thompson, *Circular code motifs in the ribosome: a missing link in the evolution of translation?*, RNA **25** (2019), 1714–1730.
- [5] E. Fimmel, S. Giannerini, D. L. Gonzalez, and L. Strüngmann, *Circular codes, symmetries and transformations*, Journal of Mathematical Biology **70** (2015), 1623–1644.
- [6] E. Fimmel, C. J. Michel, F. Pirot, J.-S. Sereni, and L. Strüngmann, *Mixed circular codes*, Mathematical Biosciences **317**, **108231** (2019), 1–14.
- [7] E. Fimmel, C. J. Michel, F. Pirot, J.-S. Sereni, M. Starman, and L. Strüngmann, *The relation between  $k$ -circularity and circularity of codes*, Bulletin of Mathematical Biology **82**, **105** (2020), 1–34.
- [8] E. Fimmel, C. J. Michel, and L. Strüngmann,  *$n$ -Nucleotide circular codes in graph theory*, Philosophical Transactions of the Royal Society A **374**, **20150058** (2016), 1–19.
- [9] E. Fimmel and L. Strüngmann, *Mathematical fundamentals for the noise immunity of the genetic code*, Biosystems **164** (2018), 186–198.
- [10] R. Grantham, C. Gautier, M. Gouy, M. Mercier, and R. Gautier, *Codon catalog usage is a genome strategy modulated for gene expressivity*, Nucleic Acids Research **9** (1981), r431–r74.
- [11] C. J. Michel, *A 2006 review of circular codes in genes*, Computers and Mathematics with Applications **55** (2008), 984–988.
- [12] ———, *The maximal  $C^3$  self-complementary trinucleotide circular code  $X$  in genes of bacteria, archaea, eukaryotes, plasmids and viruses*, Life **7** (2017), no. 2, 1–16.
- [13] ———, *The maximality of circular codes in genes statistically verified*, Biosystems **197**, **104201** (2020), 1–7.
- [14] C. J. Michel, C. Mayer, O. Poch, and J. D. Thompson, *Characterization of accessory genes in coronavirus genomes*, Virology Journal **17**, **131** (2020), 1–13.
- [15] C. J. Michel, B. Mouillon, and J.-S. Sereni, *Trinucleotide  $k$ -circular codes I: Theory*, Biosystems **217**, **104667** (2022), 1–11.
- [16] C. J. Michel and G. Pirillo, *Identification of all trinucleotide circular codes*, Computational Biology and Chemistry **34** (2010), 122–125.
- [17] C. J. Michel, G. Pirillo, and M. A. Pirillo, *Varieties of comma free codes*, Computer and Mathematics with Applications **55** (2008), 989–996.
- [18] ———, *A relation between trinucleotide comma-free codes and trinucleotide circular codes*, Theoretical Computer Science **401** (2008), 17–26.
- [19] C. J. Michel and J.-S. Sereni, *Trinucleotide  $k$ -circular codes II: Biology*, Biosystems **217**, **104668** (2022), 1–18.
- [20] ———, *Reading frame retrieval of genes: a new parameter of codon usage based on the circular code theory*, Bulletin of Mathematical Biology **85**, **24** (2023), 1–21.
- [21] C. J. Michel and J. D. Thompson, *Identification of a circular code periodicity in the bacterial ribosome: origin of codon periodicity in genes?*, RNA Biology **17** (2020), 571–583.
- [22] S. T. Parvathy, V. Udayasuriyan, and V. Bhadana, *Codon usage bias*, Molecular Biology Reports **49** (2022), 539–565.
- [23] G. Pirillo, *A characterization for a set of trinucleotides to be a circular code*, by C. Pellegrini, P. Cerrai, P. Freguglia, V. Benci, G. Israel Determinism, Holism, and Complexity, Kluwer, 2003.
- [24] V. Presnyak, N. Alhusaini, Y. H. Chen, S. Martin, N. Morris, N. Kline, S. Olson, D. Weinberg, K. E. Baker, B. R. Graveley, and J. Collier, *Codon optimality is a major determinant of mRNA stability*, Cell **160** (2015), 1111–1124.
- [25] W. Qian, J. R. Yang, N. M. Pearson, C. Maclean, and J. Zhang, *Balanced codon usage optimizes eukaryotic translational efficiency*, PLoS Genetics **8** (2012), e1002603.
- [26] K. Subramanian, B. Payne, F. Feyertag, and D. Alvarez-Ponce, *The codon statistics database: a database of codon usage bias*, Molecular Biology and Evolution **39**, **8** (2022), 1–3.

- [27] J. D. Thompson, R. Ripp, C. Mayer, O. Poch, and C. J. Michel, *Potential role of the X circular code in the regulation of gene expression*, *Biosystems* **203**, **104368** (2021), 1–15.
- [28] Z. Zhou, Y. Dang, M. Zhou, L. Li, C. H. Yu, J. Fu, S. Chen, and Y. Liu, *Codon usage is an important determinant of gene expression levels largely through its effects on transcription*, *Proceedings of the National Academy of Sciences USA* **113** (2016), E6117–E6125.